POLITECNICO DI TORINO

Master of Science in Aerospace Engineering

Master Thesis

Robust attitude control and failure analysis for small satellites.

Supervisors:

Dr. Elisa Capello

Dr. Hyeongjun Park

Candidate:

Niccolò Carnevaletti

March 2019

A mia nonna Fernanda,

Abstract

In the last years, the technological improvement and the resulting miniaturization of processors and electronics gave small satellites new capabilities and performance, previously possible only with larger satellites. As the development made possible to inexpensive and high-quality imagery as well, more satellites have been used for Earth imagery purpose and, in the next few years, this trend will not change easily. The smaller mass also allows to achieve lower launch cost, therefore giving access to space to universities and non-governmental companies. This played as a breakthrough for the entire space economy.
Since the beginning of XXI century, this increased usage led to bigger attention by customers for any kind of failure, that can affect the spacecraft at any moment. In detail, the reduced mass turns the spacecraft more sensitive to the external perturbations and the Momentum Exchange Devices (MEDs) have more limitations due to their smaller dimensions. For this reason, the key feature of the proposed research is on the design of a robust control system, able to withstand parametric uncertainties (within the plant and bounded) and matched failure of the actuation system.
The main objective is the design of an H_∞ controller, starting from Linear Matrix Inequality (LMI) formulation. This method allows achieving the required robustness, with the uncertainty derived from the unknown angular momentum of the reaction wheels and including uncertainties in the spacecraft system. The obtained controller, suitably designed for attitude control maneuver, is a "unique" state-feedback controller for both uncertainties.
The closed-loop system is evaluated for different initial conditions, including attitude positions far from the desired conditions. The effectiveness of the proposed approach is demonstrated by extensive simulations considering a pyramidal baseline configuration. Moreover, a fault detection method based on the theory of parity equation is proposed. The control law can ensure mission accomplishment in case of one wheel failed, considering a proper Fault Detection, Isolation and Recovery (FDIR) procedure. A mission scenario based on an optical Earth Observation mission is tested, in which different spacecraft configurations and failures are described.

Sommario

Negli ultimi anni, il progresso tecnologico e la conseguente miniaturizzazione di processori e componenti elettronici ha dato ai *small satellites* nuove capacità e prestazioni, possibili precedentemente solo con satelliti più grandi. Poiché lo sviluppo ha permesso anche di ottenere immagini di alta qualità a basso costo, sempre più satelliti sono usati, oggigiorno, per osservazioni legate all'ambiente terrestre e difficilmente cambierà il trend nei prossimi anni. La minore massa, inoltre, permette di avere costi di lancio meno esosi, rendendo possibile l'accesso allo spazio anche a università e compagnie non governative. Un atto senza precedenti nell'economia spaziale.
Dall'inizio del XXI secolo, questo aumento nell'utilizzo ha portato all'attenzione della comunità spaziale la maggiore vulnerabilità che questi satelliti hanno per via delle loro ridotte dimensioni. Infatti, ciò li rende maggiormente sensibili alle perturbazioni esterne e possono portare a bordo sistemi di scambio di momento (Momentum Exchange Devices o MEDs) con limitate capacità. Perciò, la caratteristica principale di questa ricerca è la progettazione di un sistema di controllo robusto che sia in grado di funzionare correttamente nonostante le incertezze parametriche, *bounded*, del sistema e malfunzionamenti del sistema attuatore. L'obiettivo principale è quindi il design di un controllore H_∞, ottenuto attraverso la formulazione delle *Linear Matrix Inequality* (LMI). Questo metodo, infatti, permette di ottenere la robustezza richiesta, considerando come incertezze del sistema il momento angolare delle *reaction wheels*, non conoscibile a priori, e le *failure* come incertezze degli attuatori. Il controllore così ottenuto, progettato specificatamente per manovre di controllo d'assetto, è un unico controllore *state-feedback* per entrambe le incertezze.
Il sistema ad anello chiuso è valutato per diverse condizioni iniziali, anche estremamente lontane dalle condizioni desiderate. L'efficacia dell'approccio proposto è dimostrata attraverso simulazioni approfondite considerando una configurazione piramidale a base quadrata. Inoltre, si propone un metodo di detezione di *fault*, basato sulla teoria delle *parity equations*. La legge di controllo garantisce la sopravvivenza della missione anche in presenza di una *reaction wheel* non funzionante, considerando una procedura *Fault Detection, Isolation and Recovery* (FDIR). Si è testato, infine, un scenario di missione, ovvero una missione di osservazione terrestre, con diversi casi di malfunzionamento.

Acknowledgement/Ringraziamenti

Firstly, I would like to thank my supervisors, prof. Hyeongjun Park and prof. Elisa Capello, for their invaluable help. For the first time, in my short academic experience, I had the unique opportunity to truly know the person beyond the chair. Thank you, I wish you all the best in your personal and working lives.
Then, I would like to thank Filippo for our shared American experience. I am writing these words in English because I know you would appreciate that. May your American dream come true, you deserve it.
È tempo di cambiare lingua e di ringraziare chi questa esperienza universitaria se l'è vissuta con me dal principio. Un sincero ringraziamento va ai miei compagni di corso, che sono stati testimoni di quanto sia "alta" la mia soglia di concentrazione. Ringrazio, in particolare, i compagni aerospaziali di sempre: Freilo, il gasator Devecchi, Simone Claudio, la parmigiana Alessia, FraGianotto, sir Daniele, il russo Artem, Rakitic e dr.10k Bongiovanni. Come dimenticare, poi, i membri del team PoliThot: il gran team leader supremo Marcolino Rotondone, Pasquale il migliore, Maurito nazionale, Frodo&Sam, il magico Andonio, il molisano, l'eroe, Cheva di Gran Burrone e tutti gli altri.
Vorrei inoltre ringraziare la gentaglia con cui ho studiato la maggior parte di questi anni. Innanzitutto, un grazie va alla mafia di Castelfidardo: Bruno, Angelo, Mimmo, Morris, Fabio, Emanuele, il Frulla, il Mazzo e Pier. Un ringraziamento va anche alle new entries dello studio matto e disperatissimo: Matteo, Alberto, Pasquale, Filippo, Robbe, Carla, Giulia e Paso.
Inoltre, vorrei ringraziare anche gli amici di sempre, sempre presenti. Grazie Melo, Enzi, Leo e anche tu, Cote. Ringrazio anche gli amici di Aosta, tra cui Alice la ragazza felice e *la cuggina* Charlotte.
Un ulteriore ringraziamento è dedicato all'ente che mi ha permesso di avere una parvenza di indipendenza economica, grazie EDISU. Sei la prova che in fin dei conti, in Italia, non è poi così male.
Infine, un ringraziamento a tutta la mia famiglia. Nello specifico, a mia nonna, per esserci sempre stata, ai miei genitori, per avermi spronato sempre e per avermi permesso di studiare *le cose intelliggenti*, e alle mie sorelle, perché così siete obbligate a ringraziare anche me nelle vostre tesi.
Last but not least, un ringraziamento alla gentil donzella Vale. Sebbene sia stato accertato che la mancanza della vena poetica non pregiudichi in alcun modo la sopravvivenza dell'individuo, la sua assenza, purtroppo, non mi permette di esprimermi nel modo in cui si dovrebbe in casi come questi, quindi la faccio semplice. Grazie per esserci stata sempre. Grazie di tutto.

Contents

List of Figures

List of Tables

Chapter 1

Introduction

Since the dawn of time, mankind has enhanced its sight towards the stars. Myths and traditions were born through the attentive observations of the sky and the creative imagination of people all around the globe. Space exploration was just a children's story, with no other purpose than letting the imagination run wild. An impossible dream until October 4^{th} 1957, when the first artificial satellite, called *Sputnik I*, was successfully launched and reached the boundaries of the space [1]. From that moment, satellites have travelled all over the solar system, even going beyond its further limits with mission *Voyager I* and *Voyager II* [2][3]. Man footsteps have already reached the lunar soil in July 20^{th} 1969 when *Apollo 11* astronauts Neil Armstrong and Buzz Aldrin became the first men reaching the moon and the day where astronauts will land on Mars is getting closer.

The first satellites were necessarily small because of reduced launch capabilities: *Sputnik I* weighted just 83 kg while *Explorer I*, the first American satellite, even less than 14 kg. As the launch technology improved, satellites acquired new dimensions and capabilities. This led to a strong decrease of the so-called small satellites launched, culminating in a *small satellite doldrums* in the 80's. This depression ended with the technological improvement and the relative miniaturization of processors and electronics, that characterized the 90's and the early 2000s. New kinds of missions were allowed thanks to the introduction of more capable payloads. Furthermore, the reduced mass, and thus a reduced launch cost, opened a new space market for universities and non-governmental companies, completely changing space industry [4].

In fact, some non-governmental companies, like SpaceX and Electron, emerged with a special focus on cutting launch cost through reusability. In December 3rd 2018, a Falcon 9 rocket (SpaceX) lifted off from Vandenberg Air Force Base, California with 64 small satellites, whose customers were from 34 different organizations [5]. Another remarkable example occurred in February 15th 2017, when ISRO's Polar Satellite Launch Vehicle successfully launched 104 satellites (103 were nanosatellites) in a single flight, breaking any previous record for the largest number of satellites launched on a single rocket[6].

Figure 1.1: PSLV-C37, when successfully lifted off with 104 satellites. Credits: Indian Space Research Organization

Since every satellite works in a harsh environment far from a direct human control, it requires a subsystem that can handle and control autonomously the attitude dynamics far from Earth. It is called *Attitude Control System*. Its main purpose is to control the orientation of the spacecraft with respect to an inertial reference frame. This subsystem includes sensors and actuators to measure the orientation and to apply the torques needed to change the orientation. The reduced dimensions, however, brought new difficulties, since small satellites are more sensitive to disturbances and perturbations than larger satellites. Therefore, a robust control is required. A first definition of robustness, although not so rigorous, can be the capability of the control system to work well under sets of parameters different from the nominal one. For example, these parameters can be uncertainties within the system, not known but bounded. In this thesis, an attitude control system is designed, to follow a pre-defined orientation, guaranteeing robustness to bounded uncertainties and external disturbances. The robust selected architecture is an H_∞ controller, able to guarantee performance through a mathematical optimization. This strategy was introduced in the '70s-'80s by George Zames[7], J.William Helton [8] and Allen Tannenbaum [9]. Another remarkable work in H_∞ methods is done by Kemin Zhou[10], in which the suboptimal H_∞ problem is explained. In the last ten years, researchers focused on Linear Matrix Inequalities (LMIs) approaches[11].

As the controller acts on the actuators through algorithms ruling the operations, it is crucial to understand the several categories of actuators used so far, analyzing their specific fields of application. In fact, several mechanisms can be used, but each case can be fitting for different scenarios. For example, thrusters are mostly used for their possible re-use for station keeping maneuvers and for their reliability in manned spacecrafts. Spin

stabilization method, where the spacecraft itself is spun up to stabilize the orientation of a single vehicle axis, is strongly used for stabilise the final stage of a launch vehicle. Then, for precise control, momentum wheels are used, where rotors, controlled by electric motors, spin to re-orient the vehicle. In case of saturation, i.e. the device reaches the maximum speed of the wheel, it is used to employ magnetorquers in presence of a magnetic field or ion thrusters. As the accuracy required in this project is remarkable, the chosen actuators are reaction wheels. However, several events have shown some vulnerabilities within these systems that can lead to serious consequences, potentially fatal for the mission. A well-known example is the mission Kepler, where two reaction wheels in a 4-configuration failed. Those failures almost cost the integrity of the mission and led NASA engineers to reformulate the mission with new constraints[12].For this reason, in this thesis, different failure cases are analyzed, to guarantee the success of the mission, even in presence of uncertainties.

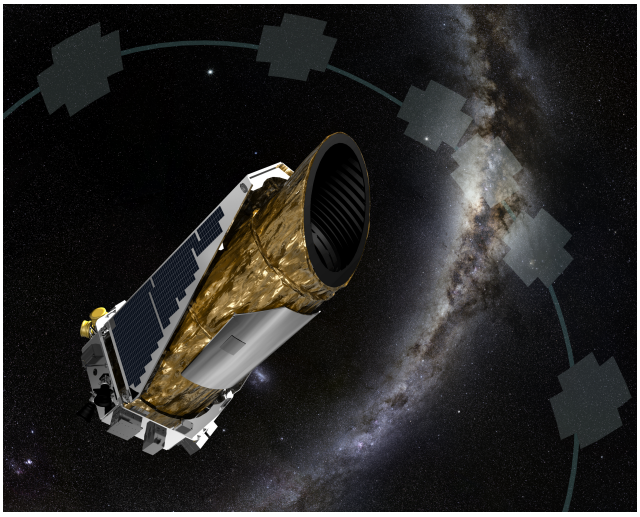

Figure 1.2: An artistic concept of Kepler, from NASA Photo Archive

In the last years, several studies considered the study of failures, including active or passive fault-tolerant methodology[13]. While the passive, due to its conservative design, has limited faults tolerance capability, the active approaches has better results, even if this method requires a Fault detection system for a complete awareness of the system in real time. An example of an adaptive attitude tracking strategy considering the fault within the controller design process is shown in [14]. In addition, a Fault-Tolerant Control (FTC) based on adaptive sliding mode have been developed by Y.Bai, J.D.Biggs, X.Wang and N.Cui[15].

1.1 Overview

As enhanced in this brief introduction, robust control methods for small satellites are getting the attention of the space systems community as they need effective approaches to withstand failures. Therefore, the aim of this thesis is to design a linear robust controller, specifically a H_∞ controller with LMI formulation, able to work well under plant uncertainties and when a failure of the actuator system occurs. The studied case is with reaction wheels as actuators in a pyramidal baseline 4-configuration. In addition, to identify in real time any failure, there has to be a fault detection method. Thus, a method based on *parity equations* approach has been chosen.

- In chapter 2, all the mathematical equations used to describe the system are shown and explained into details. The kinematics is studied with quaternions formulation to avoid singularity problem that can occur with Euler angles, while the dynamics concerned derives from the attitude problem.
- In chapter 3, a robust linear controller is described. The chosen method is an H_∞ controller, obtained through a LMI formulation. A first uncertainty, derived from the system is described.
- In chapter 4, the failure implementation is explained and tested. An assumption concerning the weight of each reaction wheels allows to consider the failure as an uncertainty.
- In chapter 5, the fault detection method used is shown. In this case, a parity equations method has been used and tested.
- In chapter 6, the controller has been tested in a real mission scenario, concerning an Earth Observation mission. The results are shown and explained in detail.
- in the last chapter, conclusion and future works are briefly discussed.

Chapter 2

Spacecraft mathematical model

In this chapter, the mathematical model is described. First, the used reference frames are described and, then, the attention will focus on the kinematics defined with quaternions and the dynamics of the satellite. Eventually, the actuator system, or Momentum Exchange Device (MED) system, is shown.

2.1 Spacecraft model

The spacecraft considered is a box of $80cm \times 80cm \times 120cm$. The weight is 200 Kg, falling within small satellite definition. In fact, according to weight and dimensions, every satellite can be classified as following:

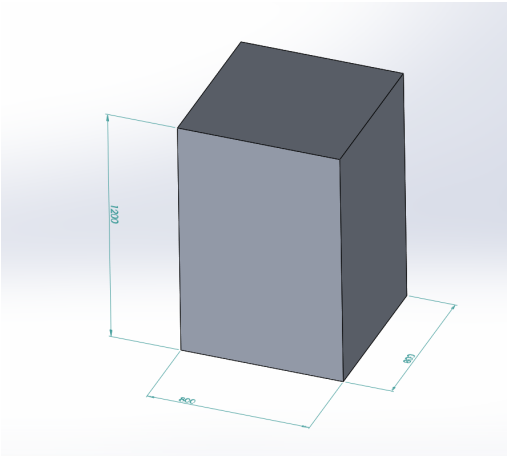

Figure 2.1: A CAD model of the spacecraft

Category	**Mass [in Kg]**
Large satellite	>1000
Medium satellite	500 to 1000
Mini satellite	100 to 500
Micro satellite	10 to 100
Nano satellite	1 to 10
Pico satellite	0.1 to 1
Femto satellite	<0.1

Table 2.1: Category of satellite

In control system engineering, it is useful to consider a dynamic system as a union of interconnecting blocks. It is therefore crucial to recreate a realistic block diagram, able to describe correctly the system. The considered case is defined as a closed-loop system, based on feedback control. It can be explained with 3 blocks: one concerning the controller, one for the system or plant and a final one for the measurements. In this thesis, it will

be considered no difference between the system output and the measured output, so the sensor part will be neglected.

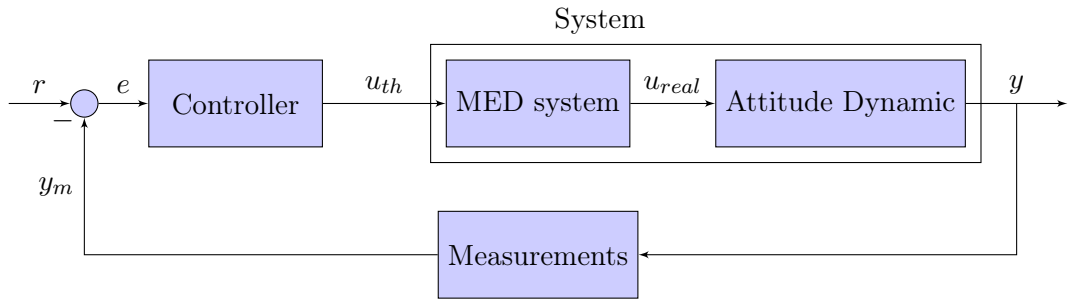

Figure 2.2: Block Diagram

2.2 Reference frames

Since the motion of a body can be described relative to a frame of reference, it is crucial to explain the used reference frames. In this thesis, it will be used an inertial frame and a body frame. The first one is a reference frame in which any body within that frame is not accelerating, if zero net force is acting upon it. Moreover, the inertial frame has the feature of being a fixed right-handed frame. Then, the body frame, corresponding to a non-inertial frame, is a moving right-handed frame centered in the spacecraft center of mass. However, these two frames, fixed and moving, are linked with each other thanks to a general property of vector, also called conversion from fixed to moving frame.

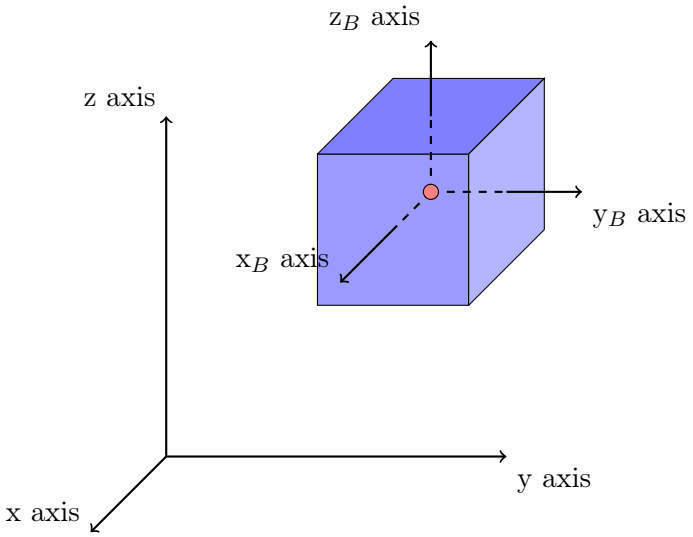

Figure 2.3: Inertial frame and body frame shown together

2.3 Attitude Dynamics with quaternions

2.3.1 Kinematics

First described by W.R. Hamilton in 1843[16], quaternions are a mathematical system extending complex numbers. Useful to describe spatial rotations due to their more compact nature, lower computational cost and their lack of singularity, they were successfully implemented in several control algorithm. A quaternion, however, can be interpreted as:

- point in a 3D projective space (w,x,y,z);
- linear transformation of four space;
- algebraic quantity;
- and a scalar plus 3-vector

In this thesis, the last interpretation is chosen and, consequently, it can be described as:

$$q = q_0 + q_1\hat{i} + q_2\hat{j} + q_3\hat{k} \tag{2.1}$$

In this thesis, it will be used a second representation too, as follows:

$$q = \begin{bmatrix} q_0 \\ q_1 \\ q_2 \\ q_3 \end{bmatrix} \quad \text{or} \quad q = \begin{bmatrix} q_1 \\ q_2 \\ q_3 \\ q_4 \end{bmatrix} \tag{2.2}$$

where q_0 and q_4 are the scalar value, while $q_{1,2,3}$ are the vector ones.
Furthermore, it is possible to describe the orientation of a rigid body through a σ rotation over an axis ν, according to Euler's theorem. Thus, considering $\vec{\nu}$ as the unit magnitude vector, quaternion can be represented as:

$$q_0 \rightarrow \cos\frac{\sigma}{2} \qquad \vec{q} \rightarrow \vec{\nu} \cdot \sin\frac{\sigma}{2}$$

For what concern quatermions, the following rules are applied:

$$\underset{ij=k=-ji}{} \qquad \underset{\substack{i^2=j^2=k^2=-1 \\ jk=i=-kj}}{} \qquad \underset{ki=j=-ik}{}$$

In addition, the quaternion norm is the following:

$$q_1^2 + q_2^2 + q_3^2 + q_4^2 = 1$$

Then, it is important to evaluate the evolution of quaternions in time. It does not go unnoticed that these equations are functions of the angular velocity.

$$\dot{q} = \frac{1}{2}\Sigma(q)\omega_B = \frac{1}{2}\Sigma(\omega_B)q \tag{2.3}$$

where

$$\Sigma(q) = \begin{bmatrix} -q_1 & -q_2 & -q_3 \\ q_0 & -q_3 & q_2 \\ q_3 & q_0 & -q_1 \\ -q_2 & q_1 & q_0 \end{bmatrix} \quad \text{and} \quad \Sigma(\omega_B) = \begin{bmatrix} 0 & -\omega_x & -\omega_y & -\omega_z \\ \omega_x & 0 & -\omega_z & \omega_y \\ \omega_y & \omega_z & 0 & -\omega_x \\ \omega_z & -\omega_y & \omega_x & 0 \end{bmatrix}$$

For ease of visualization, it is useful to know how to convert quaternions into Euler angles, as they are a more intuitive approach for displaying results.

$$\begin{bmatrix} \phi \\ \theta \\ \psi \end{bmatrix} = \begin{bmatrix} \arcsin -2(q_1 q_3 - q_0 q_2) \\ \arctan \frac{2(q_0 q_1 + q_2 q_3)}{q_0^2 + q_1^2 - q_2^2 - q_3^2} \\ \arctan \frac{2(q_1 q_2 + q_0 q_3)}{q_0^2 - q_1^2 - q_2^2 + q_3^2} \end{bmatrix} \tag{2.4}$$

2.3.2 Dynamics

Let define the total angular momentum vector as the sum of spacecraft angular momentum vector and Momentum Exchange Devices(MED) angular momentum vector.

$$h_{tot}^N = h_{s/c}^N + h_{med}^N$$

Let describe the moment equilibrium equations of a rigid body, written in an inertial reference frame.

$$\tau_{ext} = \frac{\mathrm{d}}{\mathrm{d}t}\left(h_{tot}^N\right) = \dot{h}_{tot}^N = \dot{h}_{s/c}^N + \dot{h}_{med}^N \tag{2.5}$$

where τ_{ext} is the sum of the external torques.
Let assume that $\dot{h}_{med}^N$ is equal to $-u$ where u is the control input, because equivalent to the negative torque in the body frame. Then, it is useful to convert $\dot{h}_{s/c}^N$ into body frame, considering no variation of inertia in time, i.e. $\frac{\mathrm{d}I}{\mathrm{d}t} = 0$.

$$\dot{h}_{s/c}^N = \dot{h}_{s/c}^B + \omega_B \wedge h_{s/c}^B = \cancel{\dot{I}\omega_B} + I\dot{\omega}_B + \omega_B \wedge h_{s/c}^B$$

So equation (2.5) becomes:

$$\begin{aligned} \tau_{ext} &= I\dot{\omega}_B + \omega_B \wedge h_{s/c}^B + \dot{h}_{med}^N \\ I\dot{\omega}_B &= -\omega_B \wedge h_{s/c}^B - \dot{h}_{med}^N + \tau_{ext} \\ \dot{\omega}_B &= I^{-1}\left(-\omega_B \wedge h_{s/c}^B + u + \tau_{ext}\right) \end{aligned} \tag{2.6}$$

2.4 Actuator system

Spacecraft capability of modifying its orientation arises from the use of MED systems, in particular in this thesis reaction wheels will be used. These devices apply a torque through a motor putting a wheel in rotation. Then, an equal and opposite torque is applied to the

body frame, allowing the spacecraft to rotate. It is possible to describe the behaviour of a reaction wheel through a basic model, as shown in figure 2.4. The device is composed mainly by two components: a motor and a wheel. It can be described with a local frame, referenced as the wheel frame with its spin axis aligned with the third axis.

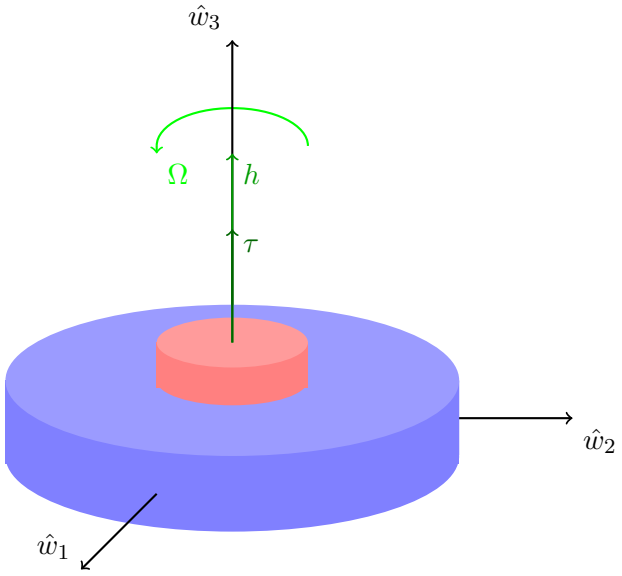

Figure 2.4: A basic model describing a reaction wheel, where the red body represents the motor and the blue body the wheel itself.

Let define the unit versors for the body frame and i^{th} wheel frame, respectively $\hat{b}_1, \hat{b}_2, \hat{b}_3$ and $\hat{w}_{i1}, \hat{w}_{i2}, \hat{w}_{i3}$. A tool fundamentals for next step is to understand how to convert from a frame to another, so it is necessary to define a transformation matrix. It can be achieved through rotations and represented as a direction cosine matrix, but for the moment it will be described just in dyadic form with component-wise dot product, as it follows:

$$ {}^{B}R^{Wi} = \begin{bmatrix} \hat{b}_1 \cdot \hat{w}_{i1} & \hat{b}_1 \cdot \hat{w}_{i2} & \hat{b}_1 \cdot \hat{w}_{i3} \\ \hat{b}_2 \cdot \hat{w}_{i1} & \hat{b}_2 \cdot \hat{w}_{i2} & \hat{b}_2 \cdot \hat{w}_{i3} \\ \hat{b}_3 \cdot \hat{w}_{i1} & \hat{b}_3 \cdot \hat{w}_{i2} & \hat{b}_3 \cdot \hat{w}_{i3} \end{bmatrix} \tag{2.7} $$

Consequently,

$$ h^{B}_{wi} = {}^{B}\, R^{Wi} h^{Wi}_{wi} \tag{2.8} $$

Focusing on angular momentum for i^{th} reaction wheel, some considerations can be done:

$$ h^{Wi}_{wi} = I^{B}_{wi}\omega^{Wi}_{wi} = \begin{bmatrix} j_{wi11} & 0 & 0 \\ 0 & j_{wi22} & 0 \\ 0 & 0 & j_{wi33} \end{bmatrix}^{Wi} \begin{bmatrix} 0 \\ 0 \\ \Omega_i \end{bmatrix}^{Wi} = \begin{bmatrix} 0 \\ 0 \\ j_{wi33}\Omega_i \end{bmatrix}^{Wi} \tag{2.9} $$

Therefore, equation (2.8) becomes:

$$h_{wi}^{B} = \begin{bmatrix} \hat{b}_1 \cdot \hat{w}_{i1} & \hat{b}_1 \cdot \hat{w}_{i2} & \hat{b}_1 \cdot \hat{w}_{i3} \\ \hat{b}_2 \cdot \hat{w}_{i1} & \hat{b}_2 \cdot \hat{w}_{i2} & \hat{b}_2 \cdot \hat{w}_{i3} \\ \hat{b}_3 \cdot \hat{w}_{i1} & \hat{b}_3 \cdot \hat{w}_{i2} & \hat{b}_3 \cdot \hat{w}_{i3} \end{bmatrix}^{Wi \to B} \begin{bmatrix} 0 \\ 0 \\ j_{wi33}\Omega_i \end{bmatrix}^{Wi}$$

$$h_{wi}^{B} = \begin{bmatrix} \hat{b}_1 \cdot \hat{w}_{i3} \\ \hat{b}_2 \cdot \hat{w}_{i3} \\ \hat{b}_3 \cdot \hat{w}_{i3} \end{bmatrix} j_{wi33}\Omega_i \tag{2.10}$$

These matrices are valid just for one reaction wheel, so it is useful to consider all the reaction wheels used. The adopted configuration is a pyramidal arrangement with 4 reaction wheels ($n = 4$). The total angular momentum of the system is simply the sum of each MED existing in the body frame.

$$h_{w}^{B} = \sum_{i=1}^{n} h_{wi}^{B} = \begin{bmatrix} \hat{b}_1 \cdot \hat{w}_{\substack{1\\3}} & \hat{b}_1 \cdot \hat{w}_{\substack{2\\3}} & \cdots & \hat{b}_1 \cdot \hat{w}_{\substack{n\\3}} \\ \hat{b}_2 \cdot \hat{w}_{\substack{1\\3}} & \hat{b}_2 \cdot \hat{w}_{\substack{2\\3}} & \cdots & \hat{b}_2 \cdot \hat{w}_{\substack{n\\3}} \\ \hat{b}_3 \cdot \hat{w}_{\substack{1\\3}} & \hat{b}_3 \cdot \hat{w}_{\substack{2\\3}} & \cdots & \hat{b}_3 \cdot \hat{w}_{\substack{n\\3}} \end{bmatrix}^{W \to B} \begin{bmatrix} h_1 \\ \vdots \\ h_n \end{bmatrix}^{W} \tag{2.11}$$

The equation (2.11) is the product of a transformation matrix $3 \times n$, where n is the number of reaction wheels, and a vector $n \times 1$ corresponding to vector column about angular momentum. It can be rewritten as:

$$h_{w}^{B} = Z^{W \to B} h_{w}^{W} \tag{2.12}$$

where

$$h_{w}^{W} = \begin{bmatrix} j_{w111} & 0 & \cdots & 0 \\ 0 & j_{w222} & \cdots & 0 \\ \vdots & \vdots & \ddots & 0 \\ 0 & 0 & \cdots & j_{wn33} \end{bmatrix} \begin{bmatrix} \Omega_1 \\ \Omega_2 \\ \vdots \\ \Omega_n \end{bmatrix}$$

Thus, the inertia matrix for reaction wheels is a $n \times n$ matrix, while the vector describing the angular rate of each reaction wheels is a $1 \times n$ vector.Then, it is important to describe analytically the MED torque, which is known to be equal to the variation in time of the angular momentum.

$$\tau_{med}^{W} = \dot{h}_{w}^{W} = I_w \dot{\Omega}_w \qquad \tau_{med}^{B} = \frac{\mathrm{d}}{\mathrm{d}t}\left(Z^{W \to B} I_w \Omega_w\right) \tag{2.13}$$

Let consider a case in which the orientation is fixed and the moment of inertia is not dependent with respect to time. So, the following is a correct assumption:

$$\tau_{med}^{B} = \cancel{\dot{Z}^{W \to B} I_w \Omega_w} + \cancel{Z^{W \to B} \dot{I}_w \Omega_w} + Z^{W \to B} I_w \dot{\Omega}_w$$

Eventually, to consider the inertial frame, equation concerning the conversion from fixed to moving frame is needed:

$$\dot{h}_{w}^{N} = \dot{h}_{w}^{B} + \omega \wedge h_{w}^{B} \tag{2.14}$$

2.4.1 Transformation matrix Z

Knowing the configuration, it is possible to evaluate the transformation matrix properly. Apart from the explaination requiring the form with component-wise dot product shown previously, it is possible to study the problem with a geometric point of view.

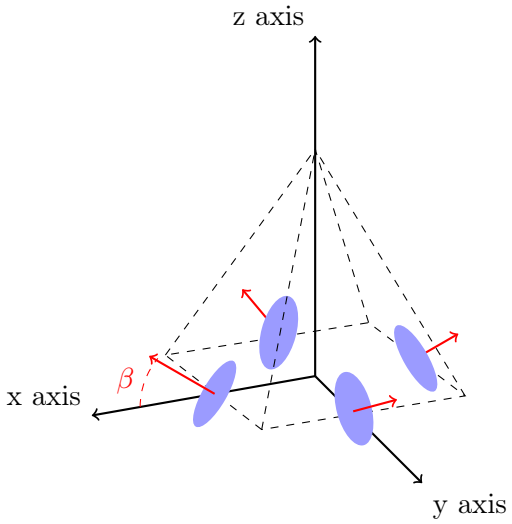

Figure 2.5: A pyramidal reaction wheel configuration, with angle $\alpha = 0°$.

Therefore, considering the angle α as the angle between $X - axis$ and the first reaction wheel and the angle β as the angle between the plane $X - Y$ and any reaction wheel assumed that every reaction wheel has the same elevation, it is possible to evaluate the angular momentum in the inertial frame starting from the reaction wheel frame:

$$
\begin{aligned}
h_x &= h_1 \cos\beta\cos\alpha - h_2 \cos\beta\sin\alpha - h_3 \cos\beta\cos\alpha + h_4 \cos\beta\sin\alpha \\
h_y &= h_1 \cos\beta\sin\alpha + h_2 \cos\beta\cos\alpha - h_3 \cos\beta\sin\alpha - h_4 \cos\beta\cos\alpha \\
h_z &= h_1 \sin\beta + h_2 \sin\beta + h_3 \sin\beta + h_4 \sin\beta
\end{aligned}
$$

Consequently, the transformation matrix is the following:

$$
Z = \begin{bmatrix}
\cos\beta\cos\alpha & -\cos\beta\sin\alpha & -\cos\beta\cos\alpha & \cos\beta\sin\alpha \\
\cos\beta\sin\alpha & \cos\beta\cos\alpha & -\cos\beta\sin\alpha & -\cos\beta\cos\alpha \\
\sin\beta & \sin\beta & \sin\beta & \sin\beta
\end{bmatrix} \tag{2.15}
$$

With $\alpha = 0°$and $\beta = 30°$, the transformation matrix used in this thesis is equal to:

$$
Z = \begin{bmatrix}
\frac{\sqrt{3}}{2} & 0 & -\frac{\sqrt{3}}{2} & 0 \\
0 & \frac{\sqrt{3}}{2} & 0 & -\frac{\sqrt{3}}{2} \\
\frac{1}{2} & \frac{1}{2} & \frac{1}{2} & \frac{1}{2}
\end{bmatrix} \tag{2.16}
$$

2.4.2 Reaction wheels saturation

A real reaction wheel has some limitations. Both the angular momentum and the maximal torque should fall within a certain range. To simulate this behaviour, better known as saturation of the reaction wheels, a specific block on SIMULINK has been used with specific data obtained by real model existing in commerce. The model considered is a Honeywell HR16-50[17].

Model	**Mass** [in Kg]	**Max Angular momentum** [in Nms]	**Max torque** [in Nm]	**Inertia** [in Kgm^2]
HR16-50	6	50	0.1	0.02

Table 2.2: Reaction wheel Data

Chapter 3

Control System Design

In this chapter, the controller used will be explained. The system is exploiting a control loop feedback mechanism control technique. The controller can be linear or nonlinear and for the purpose of this thesis a linear H_∞ is designed. The equations ruling the dynamics of a spacecraft, however, are nonlinear. It is therefore necessary to adapt the real system to a simplified mathematical model. This is achieved through a linearisation, explained in details in this chapter.

3.1 Introduction

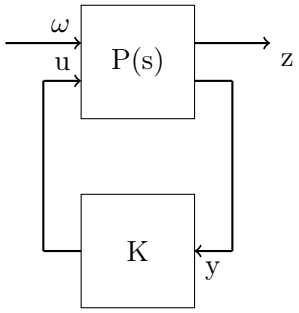

Figure 3.1: Diagram of the system, where P(s) is the open-loop system

Let consider a continuous linear time invariant (LTI) dynamical system described in a state space definition as following:

$$\begin{cases} \dot{x} = Ax + B_w w + B_u u \\ z = C_z x + D_{zw} w + D_{zu} u \end{cases} \tag{3.1}$$

where

- x is the vector state, equal to: $x = \{\vec{q}_{Error}; \vec{\omega}_{BError}\}$;

- u is the control input, equal to: $u = \{u_1; u_2; u_3\}$;
- w is the disturbance vector, equal to: $w = \{w_1; w_2; w_3\}$;
- and z is the measured output

This system, with a state-feedback controller $u = -Kx$, produces a closed-loop system as the following:

$$\begin{cases} \dot{x} = (A - B_u K)x + B_w w \\ z = (C_z - D_{zu} K)x + D_{zw} w \end{cases} \tag{3.2}$$

Which the corresponding transfer matrix from w to z is defined as:

$$\frac{Z(s)}{W(s)} = G(s) = (Cz - D_{zu} K)(sI - A + B_u K)^{-1} + D_{zw} \tag{3.3}$$

3.2 Linearisation

As mentioned before, a crucial part of the thesis was the linearisation of the equations. In order to do so, it is required to evaluate the equations (2.3) and (2.6) through a jacobian matrix, i.e. a matrix composed by all the first-order partial derivatives of a vector-valued function. However, in equation (2.3) the scalar value has to be avoided, considering hence just the vector error.

$$J = \begin{bmatrix} \frac{\partial f_1}{\partial x_1} & \cdots & \frac{\partial f_1}{\partial x_n} \\ \vdots & \ddots & \vdots \\ \frac{\partial f_m}{\partial x_1} & \cdots & \frac{\partial f_m}{\partial x_n} \end{bmatrix}$$

where

$$f = \begin{Bmatrix} \dot{q}_{Error1} \\ \dot{q}_{Error2} \\ \dot{q}_{Error3} \\ \dot{\omega}_{B1Error} \\ \dot{\omega}_{B2Error} \\ \dot{\omega}_{B3Error} \end{Bmatrix}$$

The matrices A, B_u and B_w are therefore the Jacobian matrices of the function f, with respect to x, u and w, respectively. Then, they are linearised in the neighbourhood of the equilibrium condition, which are the following:

Quaternion error	**Angular rate error** [in $\frac{rad}{s}$]
$[1, 0, 0, 0]$	$[0, 0, 0]$

Table 3.1: Equilibrium condition

For what concern C_z, D_{zu} and D_{zw}, it is possible to do the same methods, knowing the equations describing the measurements, but for the purpose of this thesis, it has been chosen to assume C_z equal to an identity matrix (6×6) and D_{zu} and D_{zw} as null matrices (6×3).

3.2.1 Matrices A, B_u, B_w, C_z, D_{zu} and D_{zw}

The matrix A is the following:

$$A = \begin{bmatrix} 0 & \frac{\omega_z}{2} & -\frac{\omega_y}{2} & \frac{q_{e0}}{2} & -\frac{q_{e3}}{2} & \frac{q_{e2}}{2} \\ -\frac{\omega_z}{2} & 0 & \frac{\omega_x}{2} & \frac{q_{e3}}{2} & \frac{q_{e0}}{2} & -\frac{q_{e1}}{2} \\ \frac{\omega_y}{2} & -\frac{\omega_x}{2} & 0 & -\frac{q_{e2}}{2} & \frac{q_{e1}}{2} & \frac{q_{e0}}{2} \\ 0 & 0 & 0 & 0 & \frac{h_{w3}}{I_1} & \frac{h_{w2}}{I_1} \\ 0 & 0 & 0 & \frac{h_{w3}}{I_2} + \omega_z & 0 & \frac{\omega_x}{2} - \frac{h_{w1}}{I_2} \\ 0 & 0 & 0 & -\frac{h_{w2}}{I_3} - \frac{\omega_y}{2} & \frac{h_{w1}}{I_3} - \frac{w_x}{2} & 0 \end{bmatrix} \tag{3.4}$$

Then, with equilibrium condition:

$$A = \begin{bmatrix} 0 & 0 & 0 & \frac{1}{2} & 0 & 0 \\ 0 & 0 & 0 & 0 & \frac{1}{2} & 0 \\ 0 & 0 & 0 & 0 & 0 & \frac{1}{2} \\ 0 & 0 & 0 & 0 & \frac{h_{w3}}{I_1} & \frac{h_{w2}}{I_1} \\ 0 & 0 & 0 & \frac{h_{w3}}{I_2} & 0 & -\frac{h_{w1}}{I_2} \\ 0 & 0 & 0 & -\frac{h_{w2}}{I_3} & \frac{h_{w1}}{I_3} & 0 \end{bmatrix} \tag{3.5}$$

The matrices B_u and B_w are the following:

$$B_u = \begin{bmatrix} 0 & 0 & 0 \\ 0 & 0 & 0 \\ 0 & 0 & 0 \\ \frac{1}{I_1} & 0 & 0 \\ 0 & \frac{1}{I_2} & 0 \\ 0 & 0 & \frac{1}{I_3} \end{bmatrix} \tag{3.6}$$

$$B_w = \begin{bmatrix} 0 & 0 & 0 \\ 0 & 0 & 0 \\ 0 & 0 & 0 \\ \frac{1}{I_1} & 0 & 0 \\ 0 & \frac{1}{I_2} & 0 \\ 0 & 0 & \frac{1}{I_3} \end{bmatrix} \tag{3.7}$$

The matrices C_z, D_{zu} and D_{zw} are the following:

$$C_z = \begin{bmatrix} 1 & 0 & 0 & 0 & 0 & 0 \\ 0 & 1 & 0 & 0 & 0 & 0 \\ 0 & 0 & 1 & 0 & 0 & 0 \\ 0 & 0 & 0 & 1 & 0 & 0 \\ 0 & 0 & 0 & 0 & 1 & 0 \\ 0 & 0 & 0 & 0 & 0 & 1 \end{bmatrix} \tag{3.8}$$

$$D_{zu} = \begin{bmatrix} 0 & 0 & 0 \\ 0 & 0 & 0 \\ 0 & 0 & 0 \\ 0 & 0 & 0 \\ 0 & 0 & 0 \\ 0 & 0 & 0 \end{bmatrix} \tag{3.9}$$

$$D_{zw} = \begin{bmatrix} 0 & 0 & 0 \\ 0 & 0 & 0 \\ 0 & 0 & 0 \\ 0 & 0 & 0 \\ 0 & 0 & 0 \\ 0 & 0 & 0 \end{bmatrix} \tag{3.10}$$

3.3 Controllability and observability

As well as a linearisation for a nonlinear system, linear controllers require the system to be controllable and observable, fundamental properties in control systems. Controllability is the ability of the system to be moved within its configuration space via a finite number of manipulations, while observability can be described as the ability of a system to let know about its internal states through external outputs.

Controllability

To evaluate the controllability, it is needed to build $n \times nr$ controllability matrix as it follows:

$$\mathcal{C} = \begin{bmatrix} B & AB & A^2B & \cdots & A^{n-1}B \end{bmatrix} \tag{3.11}$$

The system is fully controllable if the controllability matrix has full row rank, i.e. $Rank(\mathcal{C}) = n$.

Observability

For the observability, the process is similar to the controllability, thus it is needed the observability matrix:

$$\mathcal{O} = \begin{bmatrix} C \\ CA \\ CA^2 \\ \vdots \\ CA^n \end{bmatrix} \tag{3.12}$$

The system is fully observable if observability matrix has full row rank, i.e. $Rank(\mathcal{O}) = n$.

The system considered in this work has full row rank for both controllability matrix and observability matrix, thus the system is fully controllable and fully observable. Consequently, the system fulfills all the requirements for the linear controllers.

3.4 $\mathbf{H}_\infty$

Requiring a certain level of robustness, a controller has been synthesized through a H_∞ method. This family of controllers is chosen thanks to a mathematical optimization problem. In fact, the name of this method comes from the plane where the optimization is made, i.e. H_∞ is the Hardy space of matrix-valued functions. These are analytic and bounded in the open right-half of the complex plane defined by $\Re(s) > 0$, i.e. $\mathcal{RH}_\infty^+$.

Considering the LTI system in (3.1), the H_∞ norm is the induced energy-to-energy gain (induced $\mathcal{L}_2$ norm).

$$\|G\|_\infty = \|G(j\omega)\|_\infty = \sup_{\omega \in \mathbb{R}} \bar{\sigma}(G(j\omega)) \tag{3.13}$$

Unfortunately, unlike H_2 norm, H_∞ norm cannot be computed analytically. For that reason, it can be solved only with numerical methods, such as Bisection algorithm or LMI resolution. For the purpose of this thesis, the last method is chosen. However, it is possible to give a physical interpretation of this norm. In fact, it can be considered as the maximal gain of the frequency response of the system. In addiction, it can be called the worst case attenuation level as well, because it measures the maximum amplification deliverable by the system over the whole frequency set.

3.4.1 H_∞ norm computation

As previously told, numerical methods are needed. A classification can be done in this way[18]:

- **First Method**:Using a thin grid of frequency points $\{\omega_1, \cdots, \omega_n\}$,let compute Bode magnitude plot, then: $\|G(j\omega)\|_\infty \approx \max_{1 \le k \le N} \bar{\sigma}\{G(j\omega_k)\}$;
- **Second Method**:considering (3.1),$\|G\|_\infty < \gamma$ if and only if$\bar{\sigma}(D) < \gamma$ and the Hamiltonian H has no eigenvalues on the imaginary axis, where

$$H = \begin{bmatrix} A + BR^{-1}D^TC & BR^{-1}B^T \\ -C^T(I_n + DR^{-1}D^T)C & -(A + BR^{-1}D^TC) \end{bmatrix} \text{ and } \quad R = \gamma^2 - D^TD$$

- **Third Method**:(Bounded Real Lemma) The system (3.1) is internally stable and with $\|G\|_\infty < \gamma$, i.e. H_∞ performance specification, if and only if there exists a positive definite symmetric matrix **P** such that $P = P^T$ and

$$\begin{bmatrix} A^TP + PA & PB & C^T \\ B^TP & -\gamma I & D^T \\ C & D & -\gamma I \end{bmatrix} < 0, \quad P > 0$$

3.4.2 Definition of control problem

After the definition and the computation of the H_∞ norm, it is possible to define the control problem. Basically, the control objective is to minimize H_∞ norm of the transfer function from w to z. Besides, the control problem can be divided into optimal and suboptimal.
H_∞ **Optimal control problem**: Find a controller $K(s)$ able to generate a control signal u that minimizes the closed-loop norm form w to z. It aims therefore at finding the minimum value of γ.
H_∞ **suboptimal control problem**: Given a γ pre-specified, design a stabilizing controller that ensures:

$$\|G(s)\|_\infty = \max_\omega \bar{\sigma}(G(j\omega)) \leq \gamma$$

3.4.3 State feedback control problem

The method used in this thesis is a state-feedback H_∞ control, using LMIs formulation. Therefore, considering the continuous-time LTI system defined in (3.1), it is known that the control law is equal to:

$$u = -Kx \qquad \text{such that } \|G(s)\|_\infty \leq \gamma$$

Then, it is necessary to apply the bounded real lemma to the closed-loop system, trying to obtain some convex solutions.
Moreover, H_∞ performance specification written in (3.4.3) can be considered equivalent to the following linear matrix inequalities:

$$M = \begin{bmatrix} AQ + QA^T + B_uY + Y^TB_u^T & QC_z^T + \cancel{Y^TD_{zu}^T} & B_w \\ C_zQ + \cancel{D_{zu}Y} & -\gamma^2 1 & D_{zw} \\ B_w^T & D_{zw}^T & -1 \end{bmatrix} < 0 \ , \ Q > 0$$

where Q, Y and γ are the variables. The variable Q is defined as a squared matrix such that $Q = Q^T$, while the matrix Y is $(r \times n)$, with $n =$ number of vector state components and $r =$ number of control input components. These two variables derives from a linearizing change of variables, i.e. $Q = P^T$ and $Y = KP^T$ where P is such that $P = P^T$. Then, the variable γ is a scalar value.
The solution of these LMIs is processed by a mathematical solver. In this thesis, Mosek[19]

has been used, integrated on MATLAB with Yalmip[20] package. After the computation, the variables are equivalent to the final solutions, that allow to evaluate the H_∞ suboptimal state-feedback controller K as it follows:

$$K = Y_{sol} Q_{sol}^T \tag{3.14}$$

3.4.4 Uncertainties in A

A fundamental property of H_∞ controllers is their robustness with respect to uncertainties within the system. As seen in (3.5), the matrix A has some uncertainties related to the values of reaction wheels angular momentum, while the ones from the inertia matrix can be ignored in this thesis. This choice because the values of h_w will vary a lot during the simulation, as it is dependent to the control input. However, to understand how this could vary, it is necessary to look at the reaction wheels configuration used. Then, it is appropriate to analyze the working range for each reaction wheel, shown in chapter 2.4.2. Since each reaction wheel h_w^W can vary from -50 to +50, it is possible to obtain h_ω in body reference frame through the transformation matrix Z.

$$h_w^B = Z h_w^W$$

Therefore, let consider a certain number of values between -50 and $+50$ for each reaction wheel angular momentum and evaluate the corresponding A_i matrix. Therefore, it has been obtained a number of A_i matrices equal to the number of values chosen between -50 and $+50$ times 4, as the configuration of reaction wheels is with 4. Eventually, with each A_i matrix, let evaluate M_i matrices.

$$\begin{aligned} h_{wiRW1} &= \overbrace{-50, \cdots, 50}^{N \text{ values}} \\ h_{wiRW2} &= \overbrace{-50, \cdots, 50}^{N \text{ values}} \\ h_{wiRW3} &= \overbrace{-50, \cdots, 50}^{N \text{ values}} \\ h_{wiRW4} &= \overbrace{-50, \cdots, 50}^{N \text{ values}} \end{aligned} \rightarrow \begin{Bmatrix} h_{wi1} \\ h_{wi2} \\ h_{wi3} \end{Bmatrix} = Z \begin{bmatrix} h_{wiRW1} \\ h_{wiRW2} \\ h_{wiRW3} \\ h_{wiRW4} \end{bmatrix} \rightarrow$$

$$\rightarrow A_i = \begin{bmatrix} 0 & 0 & 0 & \frac{1}{2} & 0 & 0 \\ 0 & 0 & 0 & 0 & \frac{1}{2} & 0 \\ 0 & 0 & 0 & 0 & 0 & \frac{1}{2} \\ 0 & 0 & 0 & 0 & -\frac{h_{wi3}}{I_1} & \frac{h_{wi2}}{I_1} \\ 0 & 0 & 0 & \frac{h_{wi3}}{I_2} & 0 & -\frac{h_{wi1}}{I_2} \\ 0 & 0 & 0 & -\frac{h_{wi2}}{I_3} & \frac{h_{wi1}}{I_3} & 0 \end{bmatrix} \rightarrow$$

$$\rightarrow M_i = \begin{bmatrix} A_i Q + Q A_i^T + B_u Y + Y^T B_u^T & Q C_z^T & B_w \\ C_z Q & -\gamma^2 1 & D_{zw} \\ B_w^T & D_{zw}^T & -1 \end{bmatrix}$$

Eventually, to achieve an unique state-feedback controller K, the mathematical solver Mosek processes all M_i matrices through the LMI formulation, similarly as shown in the previous paragraph.

$$M_i < 0 \text{ and } Q > 0 \rightarrow K = Y_{sol} Q_{sol}^T$$

As an example, the following case is analyzed, starting from the initial conditions in terms of quaternion dynamics $q_{in} = [-0.1206, 0.4236, 0.3300, 0.8349]^T$ and in terms of angular velocity. $\omega_{Bin} = [0.0091, 0.0063, 9.754e-04]^T$.
The controller manages to effectively control the behavior of the spacecraft regardless of the initial conditions. In fact, in approximately $300s$, the spacecraft configuration is equal to $q = [0,0,0,1]^T$, $\omega = [0,0,0]^T$.

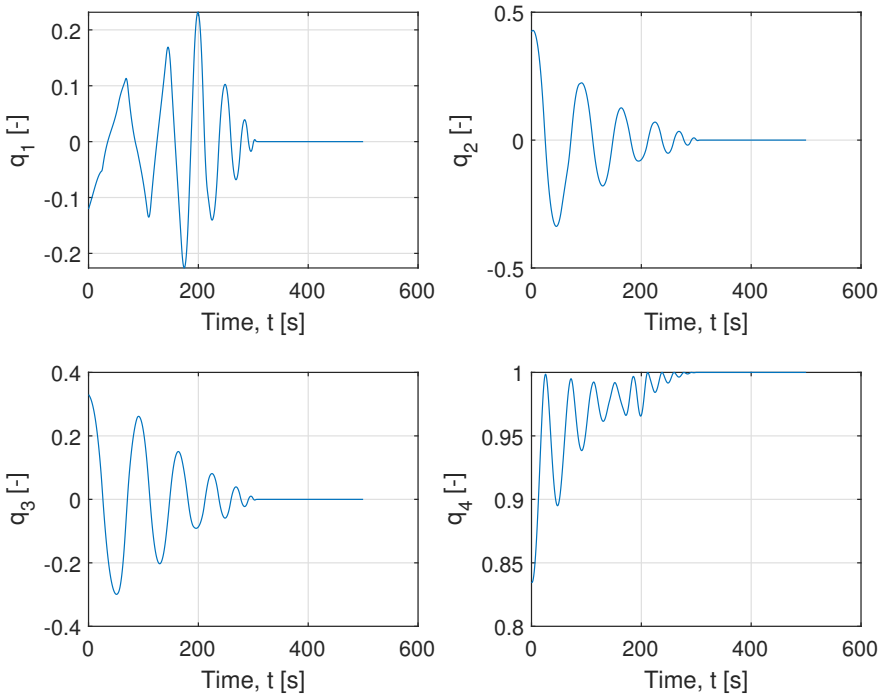

Figure 3.2: An example of quaternions variations

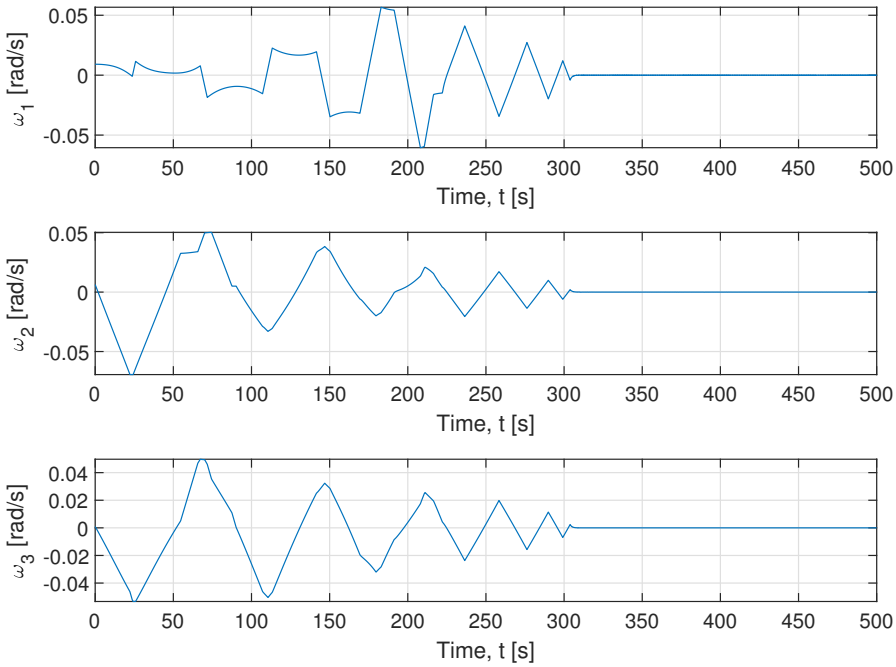

Figure 3.3: An example of angular rates variations

Chapter 4

Failure analysis

In this chapter, reaction wheels failure is analyzed and considered as an uncertainty in matrix B_u.

4.1 Failure cases

Firstly, it is necessary to define the Actuator Health Indicator matrix.

$$AHI = \Delta = \begin{bmatrix} \delta_1 & 0 & \cdots & 0 \\ 0 & \delta_2 & \cdots & 0 \\ \vdots & \vdots & \ddots & \vdots \\ 0 & 0 & \cdots & \delta_n \end{bmatrix}$$

where δ_i with $i = 1,2,\cdots,n$ indicates the status of health of the i^{th} reaction wheel. It is a scalar value between 0 and 1, where 1 represents an healthy reaction wheel while 0 a failed one.
For the sake of clarity, it is then possible to create a matrix, showing the several cases of failures. In this thesis the focus will be firstly on none failure and then on 1 RW failure with a 4 reaction wheels configuration.

$$FailureCases = \begin{bmatrix} \delta_{1_1} & \delta_{2_1} & \delta_{3_1} & \delta_{4_1} \\ \vdots & \vdots & \vdots & \vdots \\ \delta_{1_5} & \delta_{2_5} & \delta_{3_5} & \delta_{4_5} \end{bmatrix} = \begin{bmatrix} 1 & 1 & 1 & 1 \\ 0 & 1 & 1 & 1 \\ 1 & 0 & 1 & 1 \\ 1 & 1 & 0 & 1 \\ 1 & 1 & 1 & 0 \end{bmatrix}$$

where each row is equivalent to the diagonal components of AHI matrix and each column represents δ_i, where i is the column, for the several cases. Thus, all AHI matrices are well defined.

4.2 B uncertainties

It is possible to rewrite the dynamic equations, through the Actuator Health Indicator, as the following:

$$I\dot{\omega} = -\omega \times (I\omega + h_\omega) + Z \cdot \Delta \cdot T_{wheel} + T_{disturbances}$$

In the nominal case, the jacobian matrix of these equations with respect to the control input u would be like $B_u = [0_{3x3}; I_{s/c}^{-1}]$ so it is verified that the derivative of $Z \cdot \Delta \cdot T_{wheel}$, with respect to u, is equal to $[1; 1; 1]$. This is obtained by 4 Reaction wheels working, so it is possible to understand the weight of each reaction wheel, knowing the configuration.

Consequently, in nominal case, there is

$$Z \cdot \begin{bmatrix} \tau_1 \\ \tau_2 \\ \tau_3 \\ \tau_4 \end{bmatrix} = \begin{bmatrix} 1 \\ 1 \\ 1 \end{bmatrix}$$

A problem occurs as the transformation matrix Z is not squared and not invertible. However, in linear algebra, there exists a generalization of inverse matrix, called Moore-Penrose inverse or, more usually, pseudoinverse. For the purpose of this thesis, it will be used the MATLAB function *pinv*. So, the weights of each reaction wheel are the following:

$$\tau = Z^+ \cdot 1_{3x1}$$

In nominal case, $Z \cdot \Delta \cdot \tau = Z \cdot \tau$ is verified, so

$$\frac{Z \cdot \Delta \cdot \tau}{Z \cdot \tau} = 1$$

In case of failure, this ratio would not be equal to 1, but it represents the uncertainty we are looking for. So, in the most general case, it is possible to rewrite the matrix B_u in the following way:

$$B_u = \begin{bmatrix} 0 & 0 & 0 \\ 0 & 0 & 0 \\ 0 & 0 & 0 \\ I_{s/c_X}^{-1}(uncertainty(1)) & 0 & 0 \\ 0 & I_{s/c_Y}^{-1}(uncertainty(2)) & 0 \\ 0 & 0 & I_{s/c_Z}^{-1}(uncertainty(3)) \end{bmatrix}$$

where $uncertainty = \frac{Z \cdot \Delta \cdot \tau}{Z \cdot \tau}$.
In the simulation, the allocation torque matrix used will be the following:

$$Z = Z_{geometric} \cdot \Delta$$

So, as shown for A's uncertainties, for each case it will be necessary to build matrices M_i and then generate a single state-feedback controller K.

4.3 Nominal and failure cases

The initial conditions are the following:

q_{in}	-0.1206	0.4236	0.3300	0.8349 (scalar)
$\omega_{B_{in}}$	0.0091	0.0063	$9.7540 \cdot 10^{-4}$	

In the following case, the nominal system is analyzed, in which no failures are considered.

As it is possible to notice, the controller achieves the convergence of the solution within $300s$. This solution is almost equal to the one obtained by the controller made without B_u uncertainty, shown in 3.3. In fact, the initial conditions are the same for both cases.

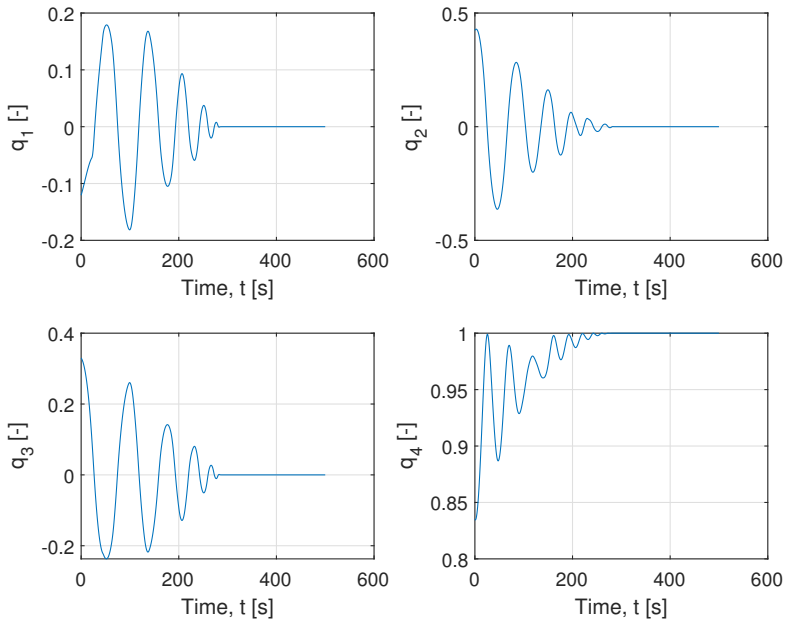

Figure 4.1: Quaternions behaviour with no failure

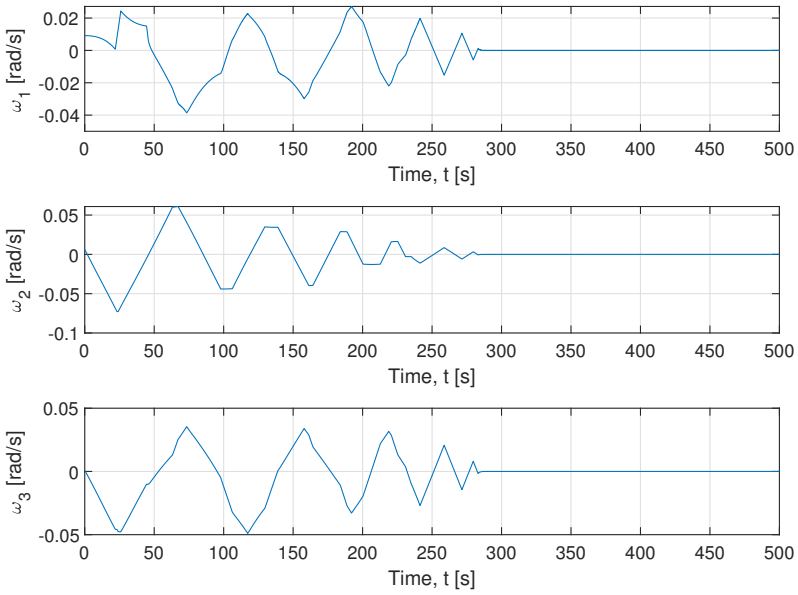

Figure 4.2: Angular rates behaviour with no failure

Then, the case concerning the first reaction wheel failed is shown:

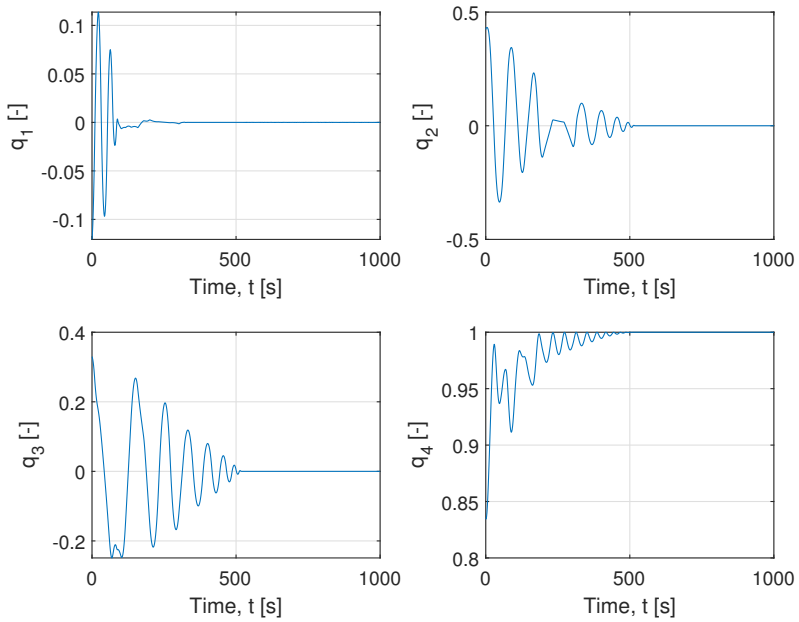

Figure 4.3: Quaternions behaviour with 1^{st} Reaction wheel failed

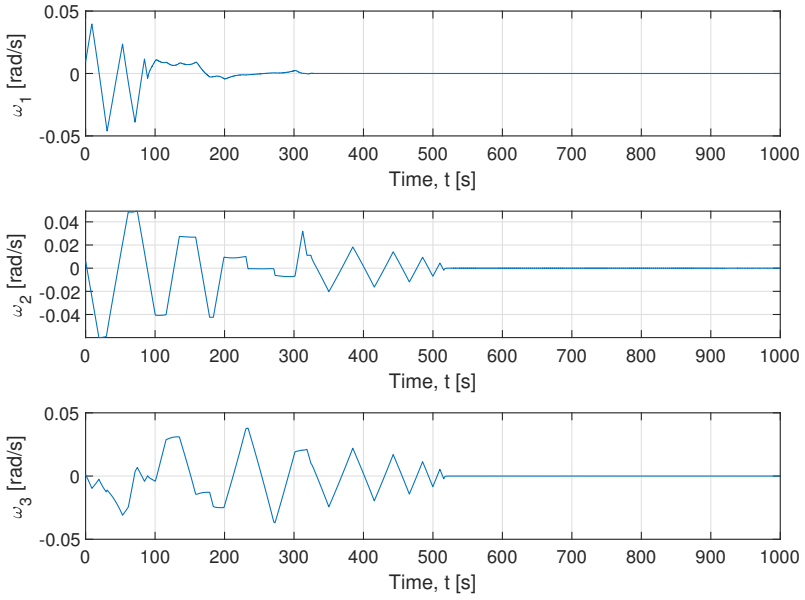

Figure 4.4: Angular rates behaviour with 1^{st} Reaction wheel failed

Due to the failure of the first reaction wheel, the controller requires more time than the nominal case to achieve the optimal control, obtained in approximately $520s$. The time spent in maneuvering is almost three-quarters more. It is, however, acceptable for this kind of satellite.

Next, the case with the second reaction wheel is considered.

The failure of the second reaction wheel is more complicated to control for the controller. Although the initial conditions are the same, the desired configuration is obtained in approximately $910s$. This different behavior can be explained through the different weight that each reaction wheel has. As it is seen previously in this chapter, the work done by each reaction wheel is not equally divided.

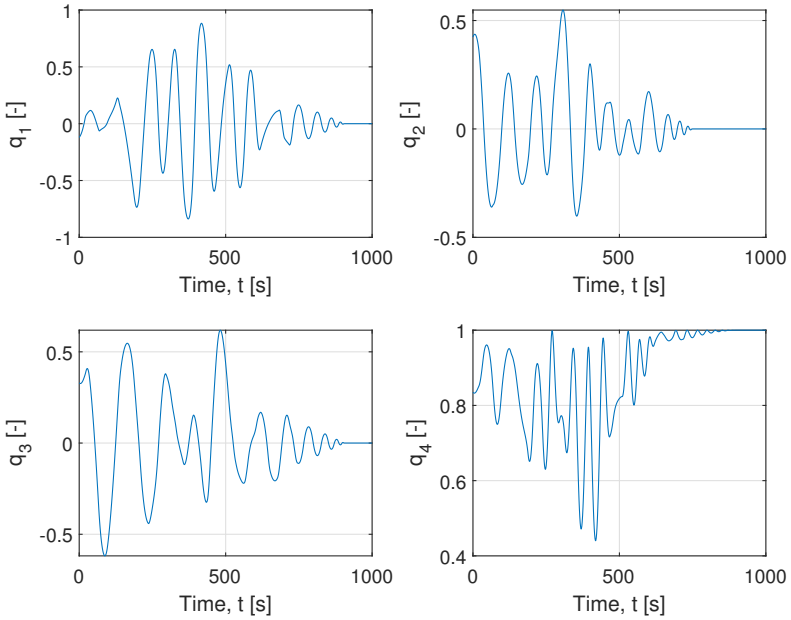

Figure 4.5: Quaternions behaviour with 2^{nd} Reaction wheel failed

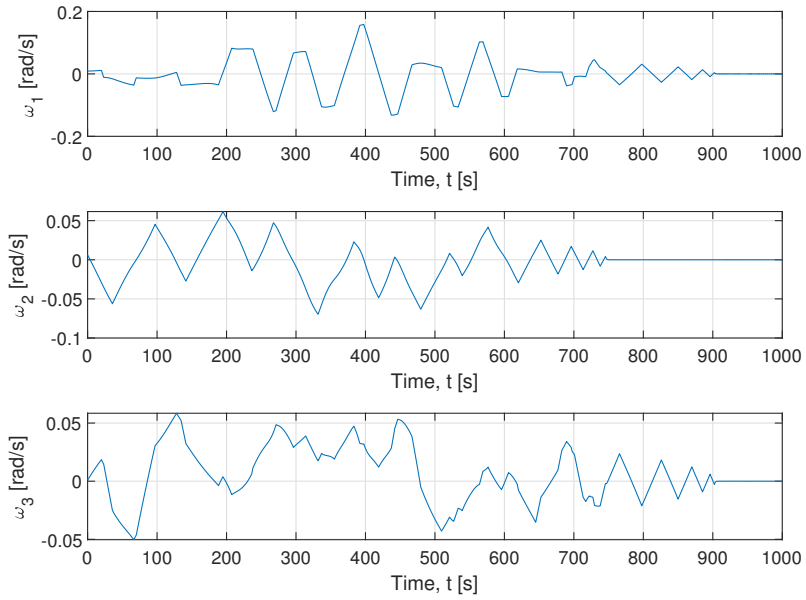

Figure 4.6: Angular rates behaviour with 2^{nd} Reaction wheel failed

The third case is analyzed and shown in figure4.7.

For what concern the failure of the third reaction wheel, the behavior is very close to the nominal case, even better. In fact, the controller achieves the desired configuration in less than $300s$, spending less time than the nominal case.

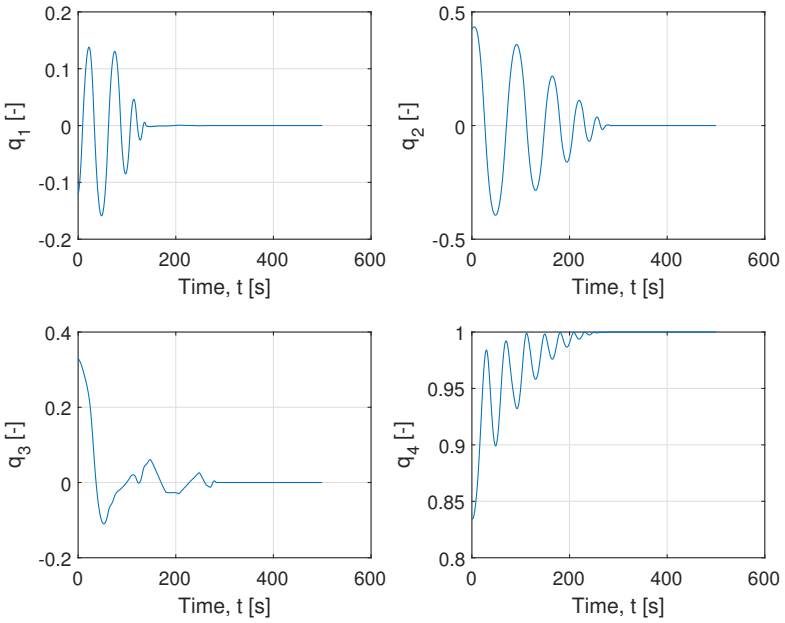

Figure 4.7: Quaternions behaviour with 3^{rd} Reaction wheel failed

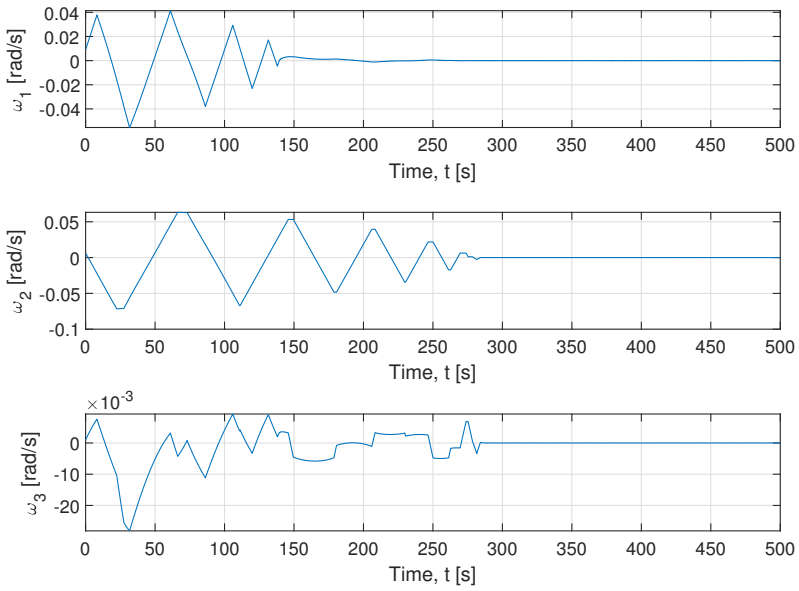

Figure 4.8: Angular rates behaviour with 3^{rd} Reaction wheel failed

The fourth case is presented in the following figures 4.9 & 4.10.

The consequences of the failure of the fourth reaction wheel lead the controller to delay the achievement of the desired configuration of almost $80s$, keeping however a good behavior. Therefore, the control maneuver lasts for approximately $380s$.

In Conclusion, it is possible to affirm that the controller with these initial conditions can always manage a reaction wheel failure within an acceptable time. However, it is clear that the behavior is different according the kind of failure.

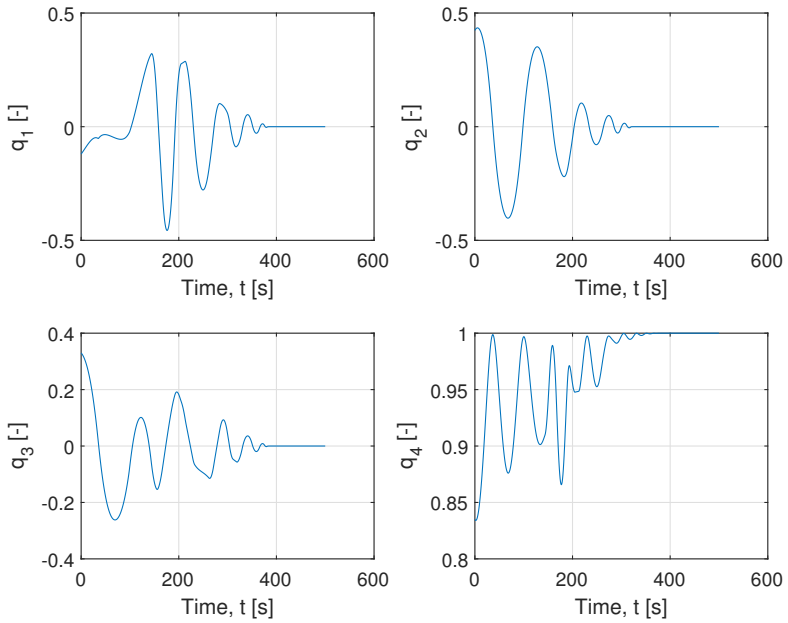

Figure 4.9: Quaternions behaviour with 4^{th} Reaction wheel failed

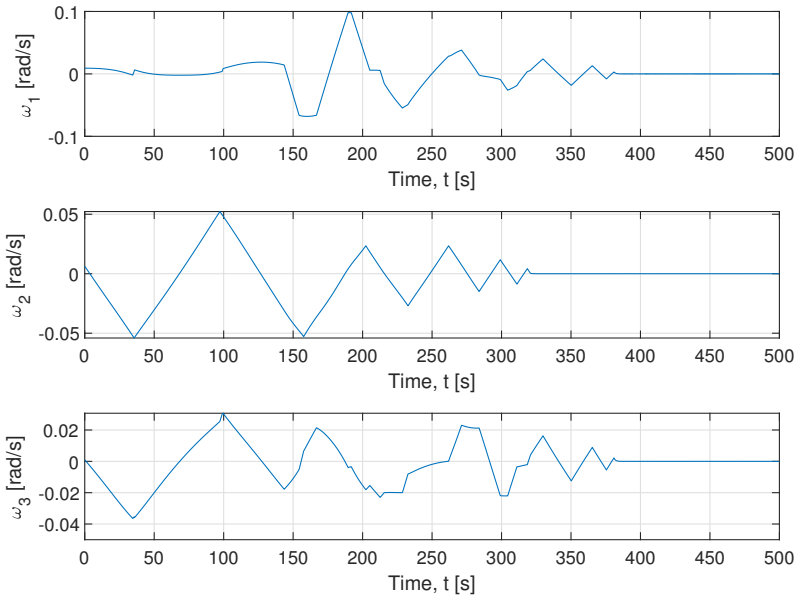

Figure 4.10: Angular rates behaviour with 4^{th} Reaction wheel failed

4.4 Effectiveness of the failure assumption: comparison between controllers

In order to validate the assumption made and the real effectiveness of it, the work focused on the comparison of two different controller: the first one made with only the uncertainty derived from the system, the second one that considers, as well, the uncertainty of the matrix relative to the actuators, i.e. B_u matrix. Therefore, a MATLAB script has been written, able to compare autonomously the two different controllers with several initial conditions. An example that well represents the behaviors of these controllers is shown in the following sections.
The example considered has the following initial conditions:

q_{in}	-0.0641	0.3897	0.3093	0.8650 (scalar)
$\omega_{B_{in}}$	0.0049	0.0045	0.0065	

The nominal case is shown, where no failure is affecting the actuator system.

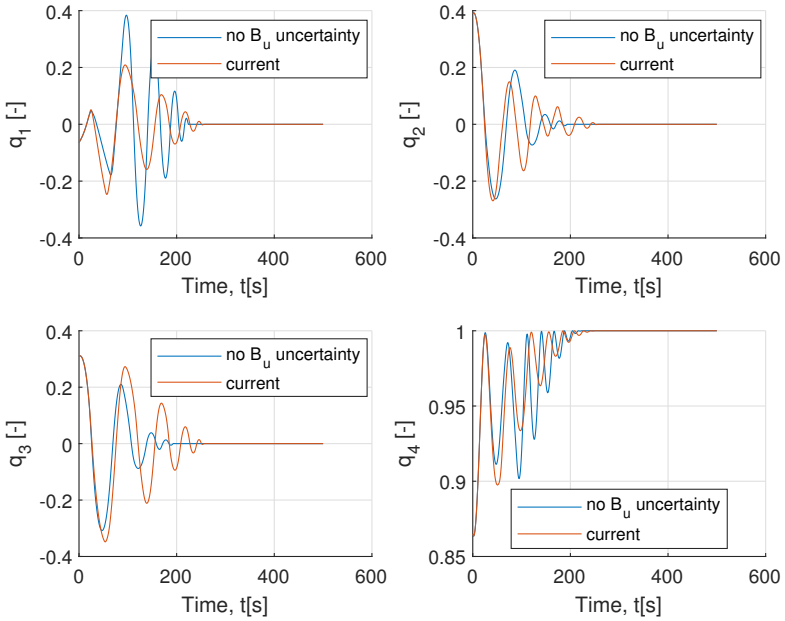

Figure 4.11: Quaternions behaviour with none Reaction wheel failed

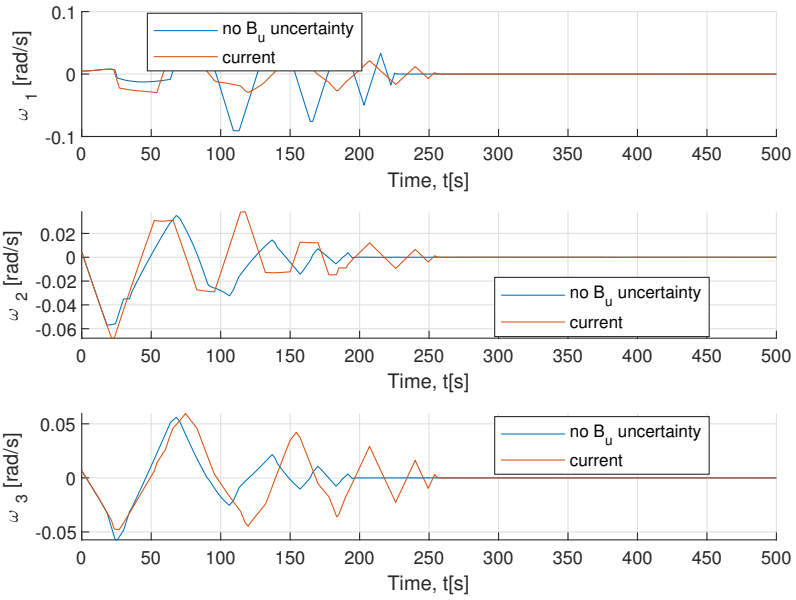

Figure 4.12: Angular rates behaviour with none Reaction wheel failed

The nominal case shows no big differences. However, the controller made without the assumption achieves the control in less time than the current controller. This behavior is explained because the first controller was designed considering only the nominal case. The first controller reaches the final configuration in approximately $225s$, while the second in approximately $250s$.

Then, the first reaction wheel failed is considered, so the simulation is the following.

The effectiveness of the assumption is clear: with the first reaction wheel failed, the basic controller cannot achieve a control in less than $5000s$, while the second can achieve it in less than $500s$. The difference is not neglectable and the assumption is a key factor for the controller success.

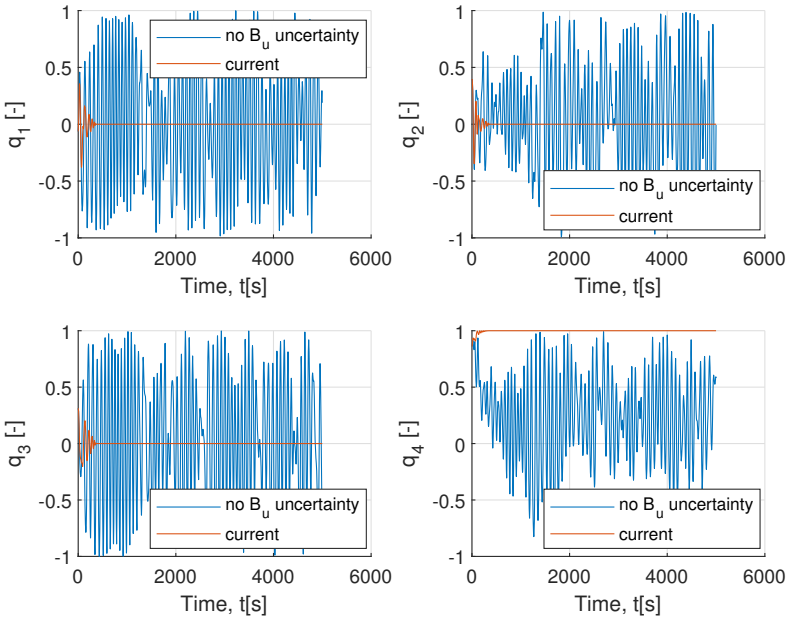

Figure 4.13: Quaternions behaviour with 1^{st} Reaction wheel failed

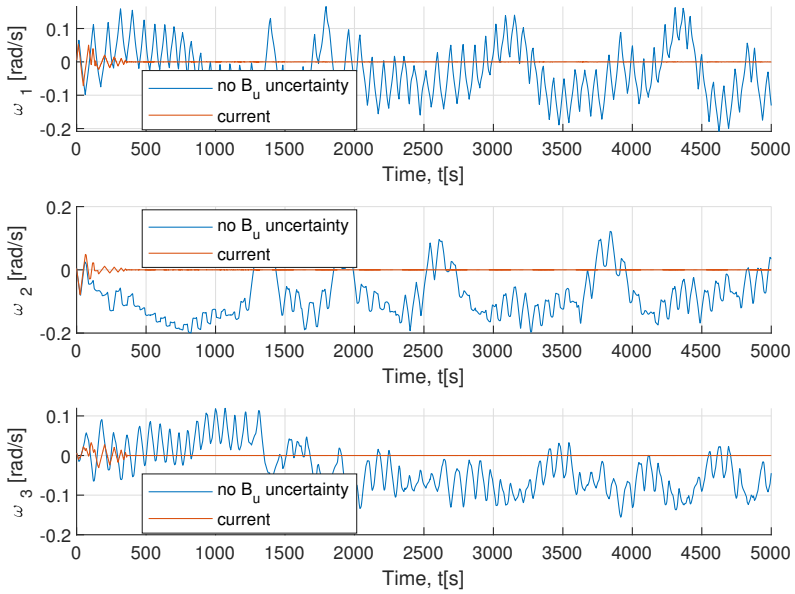

Figure 4.14: Angular rates behaviour with 1^{st} Reaction wheel failed

Next, it is analyzed the failure of the second reaction wheel. The simulation is the following.

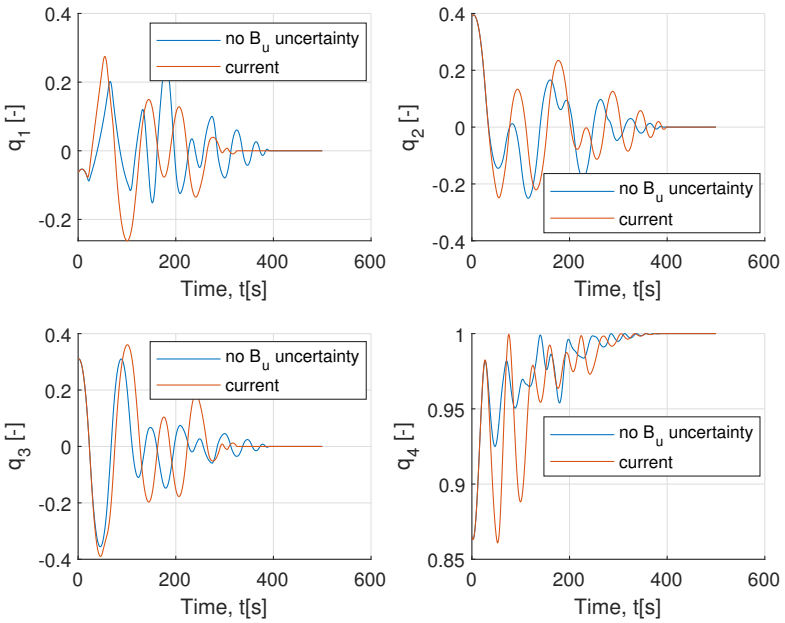

Figure 4.15: Quaternions behaviour with 2^{nd} Reaction wheel failed

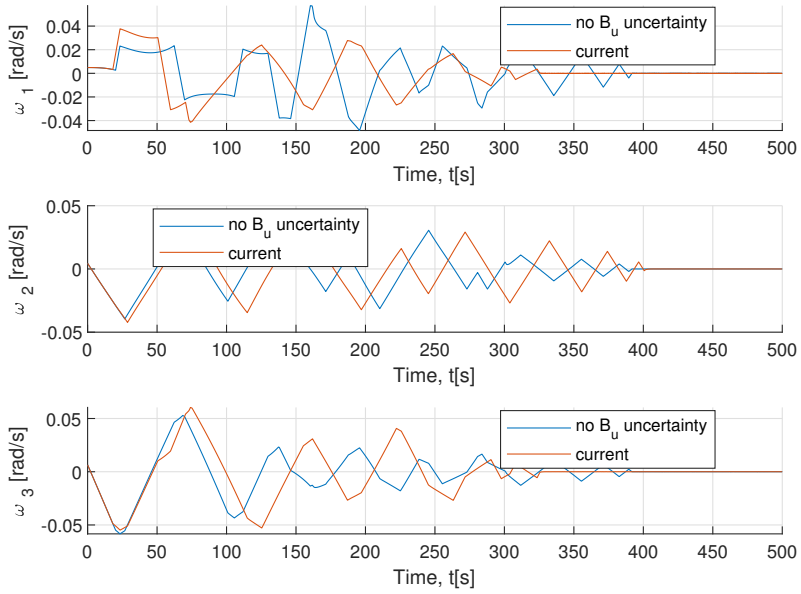

Figure 4.16: Angular rates behaviour with 2^{nd} Reaction wheel failed

Both controllers behave in almost the same way. They reach the desired configuration in approximately $400s$, with the first controller slightly earlier. However, the difference is neglectable. In addition, it can be seen that the behavior of the second controller is always within $500s$.

The case concerning the third reaction wheel failed is now presented.

The third reaction wheel failed leads to a behavior like what seen during the first reaction wheel failure. In fact, the first controller cannot achieve the desired configuration in $5000s$, while the second successfully concludes the maneuver in less than $500s$. the assumption is still a key factor for the maneuver success.

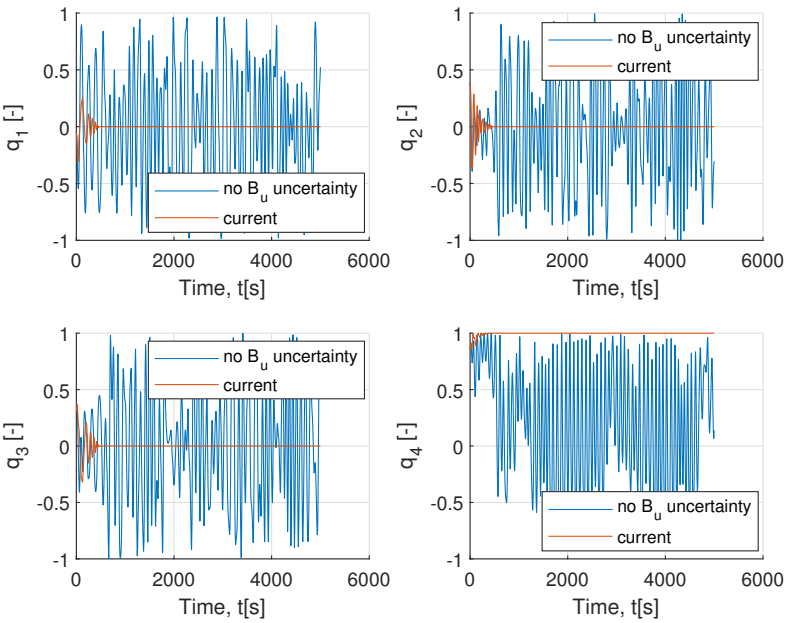

Figure 4.17: Quaternions behaviour with 3^{rd} Reaction wheel failed

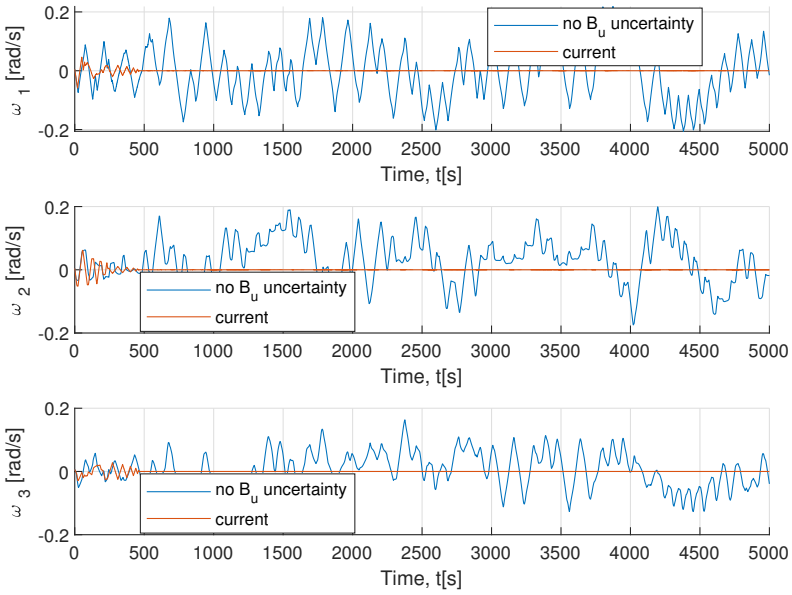

Figure 4.18: Angular rates behaviour with 3^{rd} Reaction wheel failed

Finally, the case with the fourth reaction wheel failed is analyzed. The simulation gives the following results:

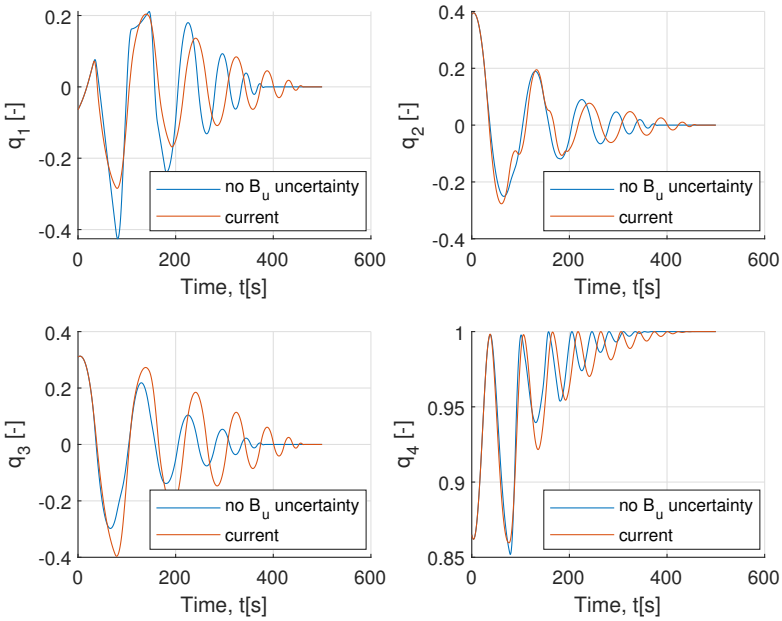

Figure 4.19: Quaternions behaviour with 4^{th} Reaction wheel failed

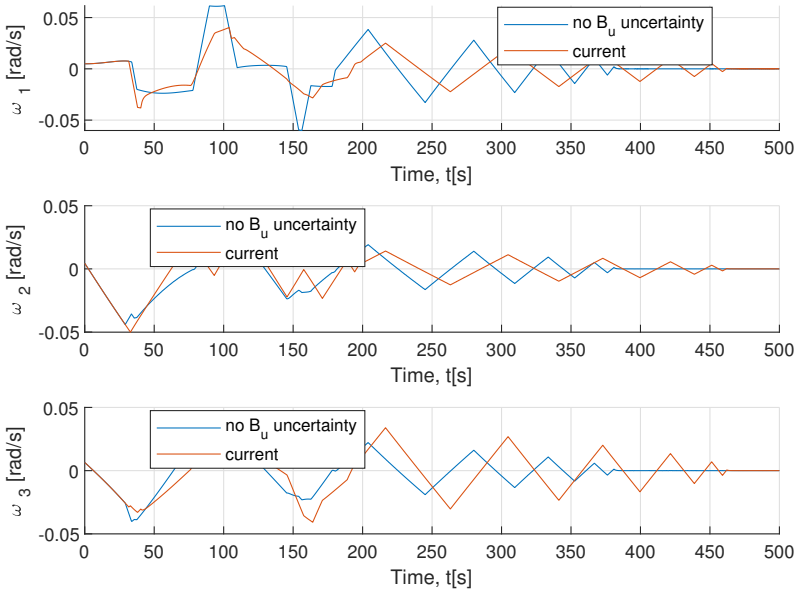

Figure 4.20: Angular rates behaviour with 4^{th} Reaction wheel failed

In the case showing the fourth reaction wheel failed, the behavior of both controllers is similar, with the first controller achieving the equilibrium almost $100s$ earlier. The desired configuration is achieved in less than $400s$ for the first controller and approximately in $450s$ for the second controller.

To sum up, the controller made without assumption is more sensitive to failure, showing an inability to achieve the desired configuration during the first and the third reaction wheel failures. As well as the effectiveness of the assumption made, it is proven the capability of the controller to achieve the equilibrium in a range of acceptable time with these initial conditions.

Chapter 5

Fault Detection Methods

In this chapter, the fault detection method is presented. Since the spacecraft requires a high level of reliability and safety of technical plants, it is crucial to have a complete awareness of the system in real-time. Therefore, an early detection of process faults is needed. By literature, it is possible to find several methods, that can be, however, summed up into three main groups [21]: *Data Methods and Signal Models*, exploiting available data from previous experiments; *Process Model Based Methods*, based on analytical redundancy concept, and *Knowledge Based Methods*, concerning artificial intelligence and rule-based expert methods. For what concern this project, a *Process Model Based Method* has been chosen, specifically a *Parity equations* approach.

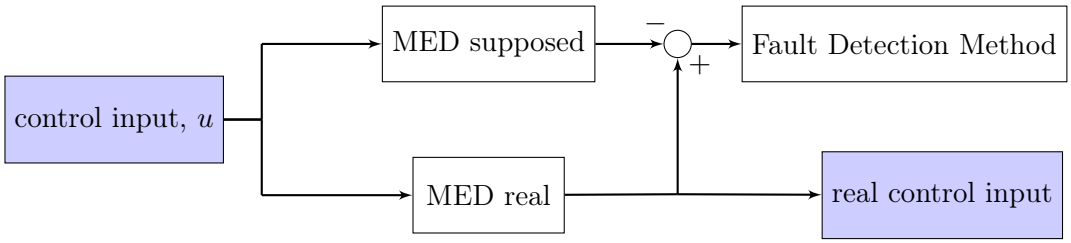

Figure 5.1: MED system and Fault Detection system

5.1 Parity equations

This method is based on the concept of the analytical redundancy. Basically, it requires to compare two systems, ruled by the same equations, where one is not affected by any failure. Thus, the redundant nominal system and the real system receive the same input signal, but the output signals may not coincide as the real system can be affected by failures. The discrepancies of the output signals are then analyzed and can detect the specific position of the failure.
As this thesis focuses on actuators failure, the system required for the redundancy is the

MED system. To well describe the failure, as previously told in chapter.4, it can be represented as a control allocation torque matrix problem. More specifically, for the nominal system, this matrix is always equal to the geometric transformation matrix $Z_{geometric}$ and, thus, independent to failures. For the real system, the geometric transformation matrix is multiplied by the control allocation torque, as shown in chapter.4.

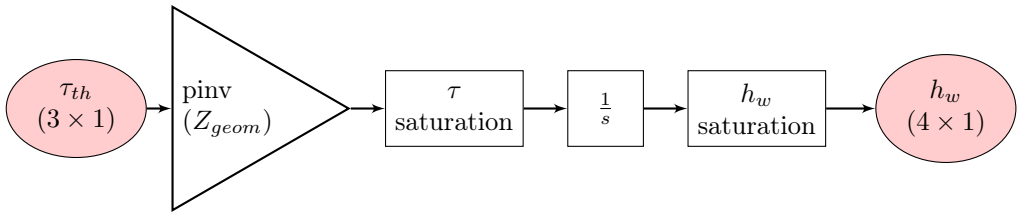

Figure 5.2: Nominal MED system

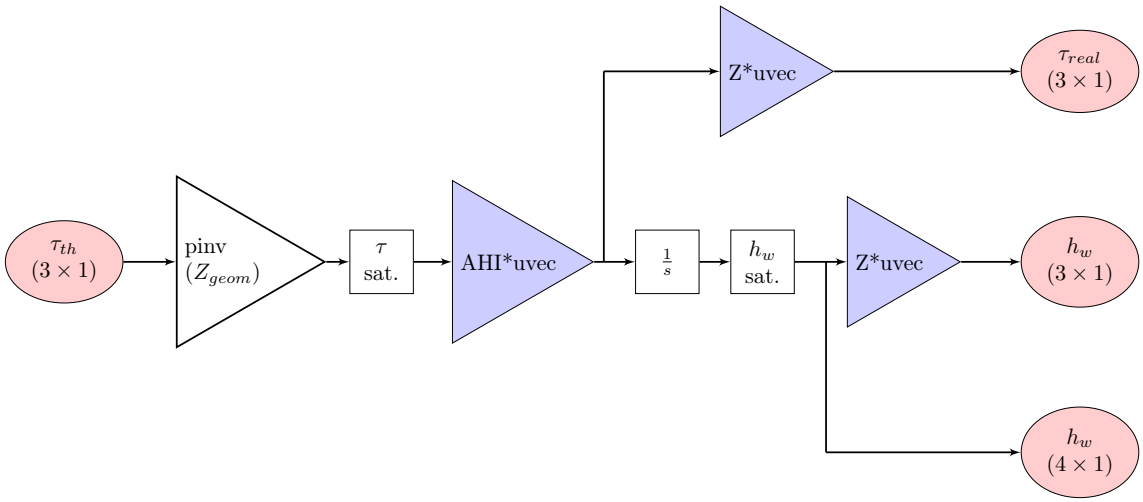

Figure 5.3: Real MED system, where blue blocks are the one affected by the failure and *sat.* is for saturation.

Focusing on the MED systems, in order to detect the failure, it has been chosen to compare the angular momentum h_{wi} of each reaction wheel for both systems. Through a simple subtraction of these values, it is possible to understand the behavior for each device. In fact, if there is any difference, the reaction wheel is failed, else it is healthy. To ease the understanding, the health condition is shown graphically in 5.4, where 0 is equal to healthy reaction wheel and 1 to failed reaction wheel.
However, the system concerning the description of the spacecraft attitude requires reaction wheels angular momentum with respect to the inertial frame, while for the right functioning of the fault detection method a wheel frame is required. For that reason, it is possible to notice a change of reference frame in the last part of the real system.

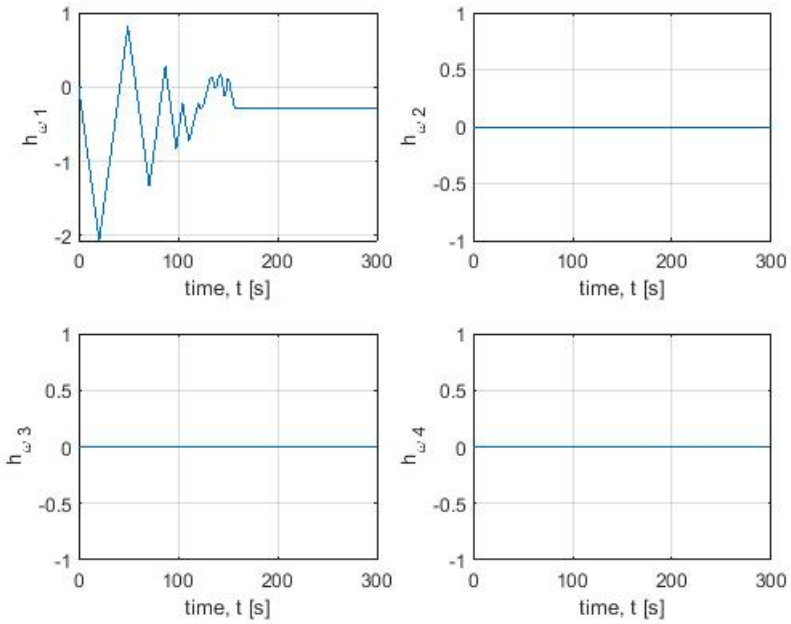

Figure 5.4: h_w differences, with 1^{st} reaction wheel failed

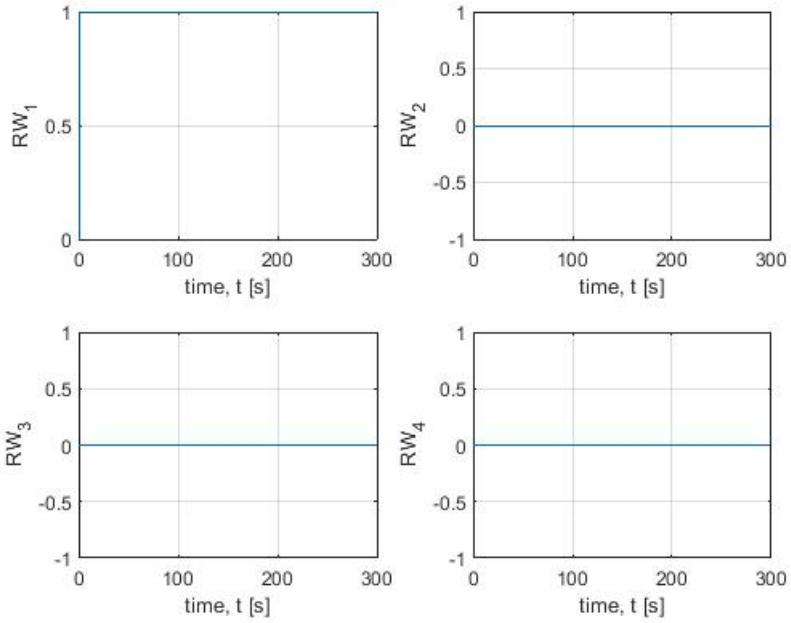

Figure 5.5: Fault visualization, with 1^{st} reaction wheel failed

Chapter 6

Mission Scenario

As introduced in the first section of this thesis, small satellites are living a revival in these last few years and they are acquiring a whole new kind of missions. Due to the strong increase of imagery capabilities, it is now possible to plan an Earth observation mission even with satellites whose mass is less than 300 Kg. Therefore, to verify the reliability and the robustness of the designed controller, a real mission scenario concerning an Earth Observation has been tested for 5 cases: one with no reaction wheel failure and the other 4 with a reaction wheel failure, one for each reaction wheel failed considering a pyramidal baseline RW-configuration.

6.1 Desired configuration

As the controller works with the error, i.e. the difference between the reference and the output, that should be kept zero or, at least, very small, it is important to define the right reference. For this mission, an example of desired quaternions and angular rates are proposed in the following figures. The whole mission lasts 86400s, equal to one civil day, but the actual maneuver occurs in 695s starting after 83984s. Therefore, only the part concerning this maneuver is shown, as the remaining parts always keep the same configuration. Moreover, the maneuver can be described in three phases. Firstly, there is a transitional phase, where the spacecraft moves from the initial configuration to the desired configuration. Then, a scientific phase occurs, in which the spacecraft moves according the mission chosen path. Finally, the spacecraft returns to its initial configuration after a second transitional phase.

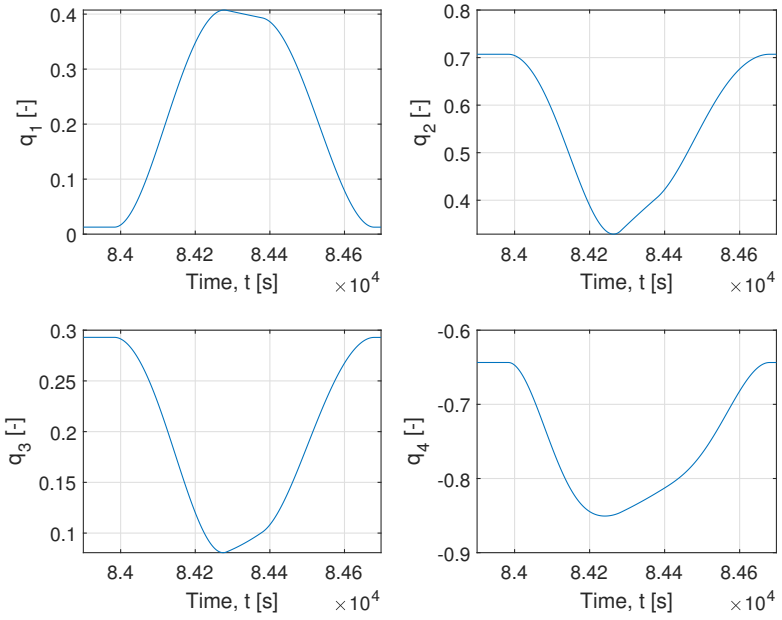

Figure 6.1: Desired quaternions

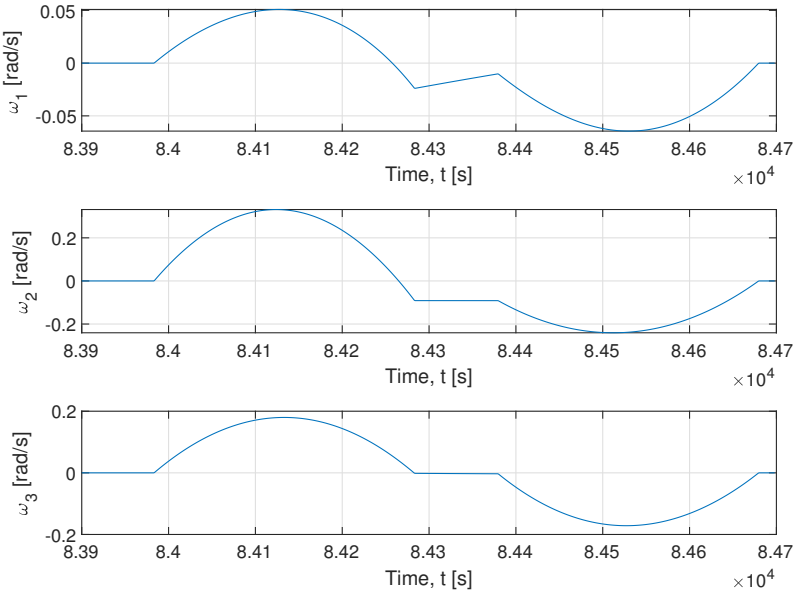

Figure 6.2: Desired angular rates

6.2 Resulting mission scenario with designed controller

The nominal case is analyzed and the next figures show the behaviors of quaternions and angular rates compared to the desired ones and their relative errors.

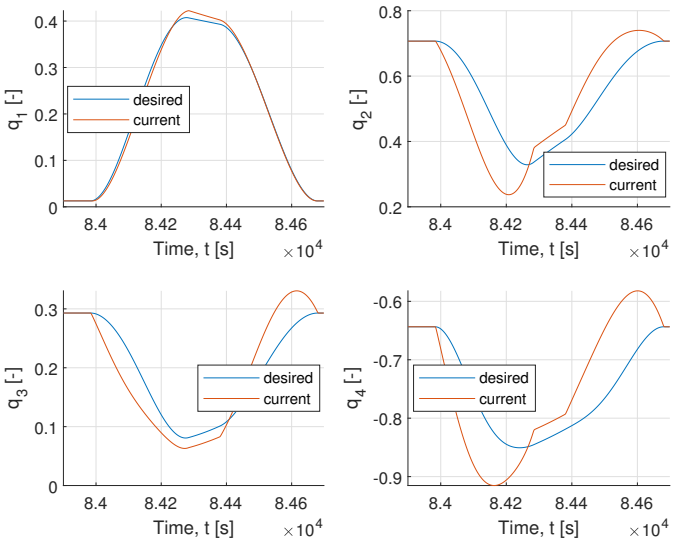

Figure 6.3: Quaternions, no failure

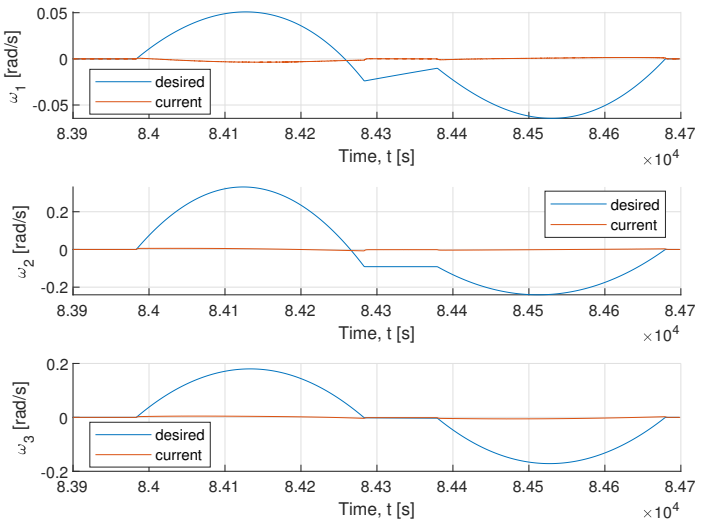

Figure 6.4: Angular rate, no failure

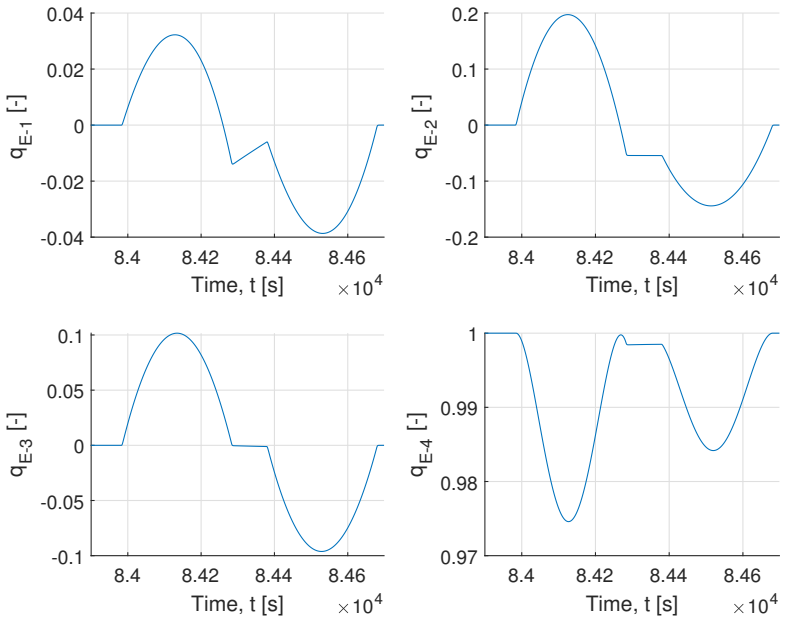

Figure 6.5: Quaternion error, no failure

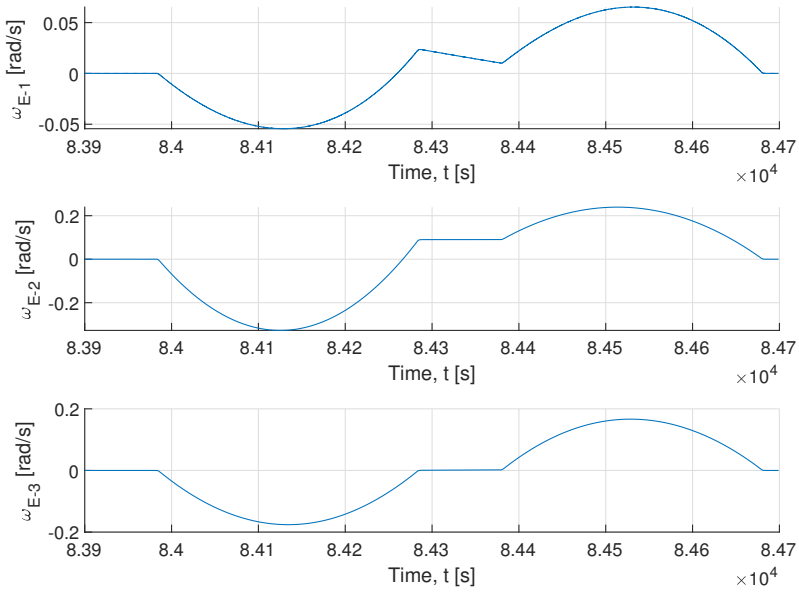

Figure 6.6: Angular rate error, no failure

The simulation shows a controller that struggles trying to follow the desired configuration, especially during the transitional phases. In these parts, the errors are important, but they are more acceptable in the scientific phase, where the errors should be minimized. The quaternion q_1 is really close to the desired one, while the others, q_2, q_3 and q_4, present an overshooting problem. The angular rates seem to not be affected by the controller.

Then, the case concerning the first reaction wheel failed is considered.

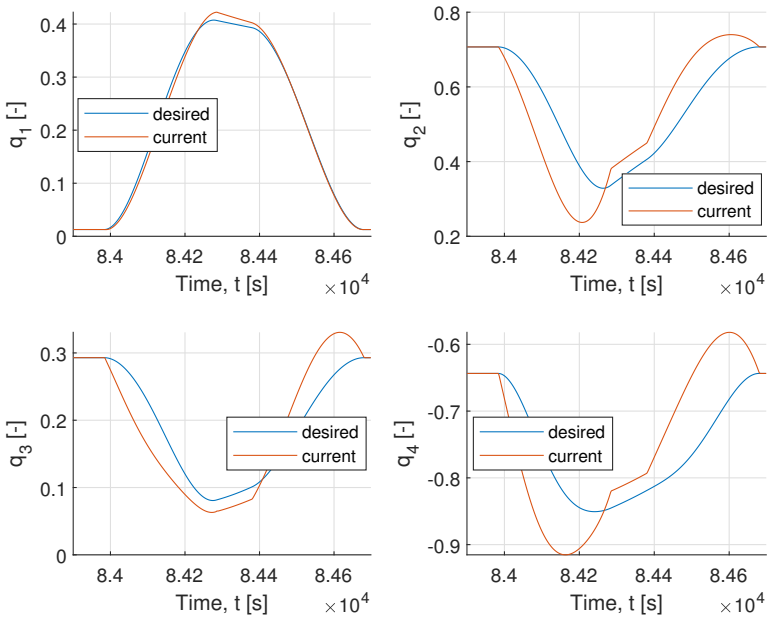

Figure 6.7: Quaternions, 1^{st} reaction wheel failed

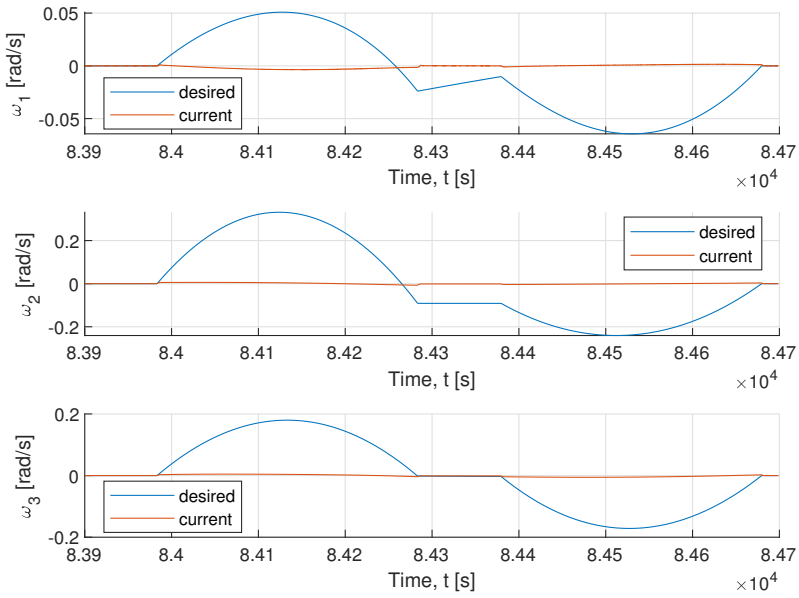

Figure 6.8: Angular rate, 1^{st} reaction wheel failed

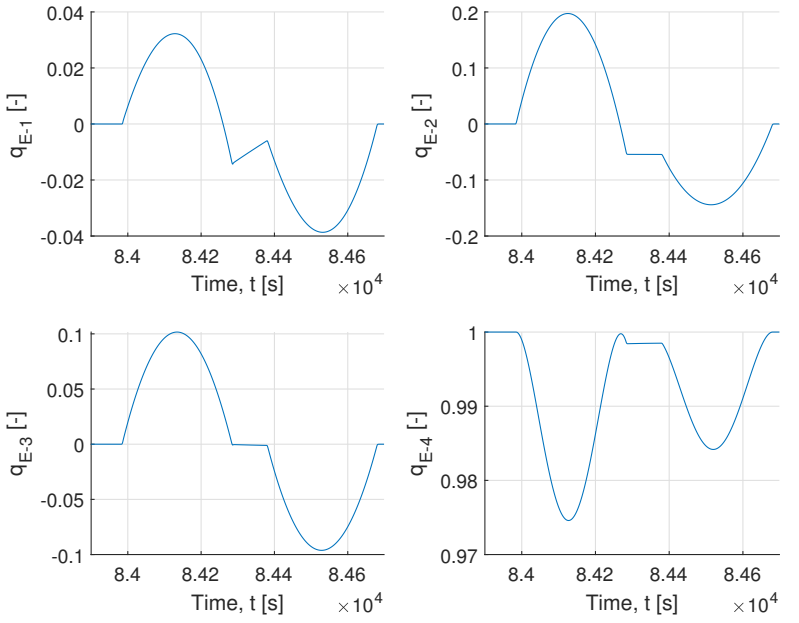

Figure 6.9: Quaternion error, 1^{st} reaction wheel failed

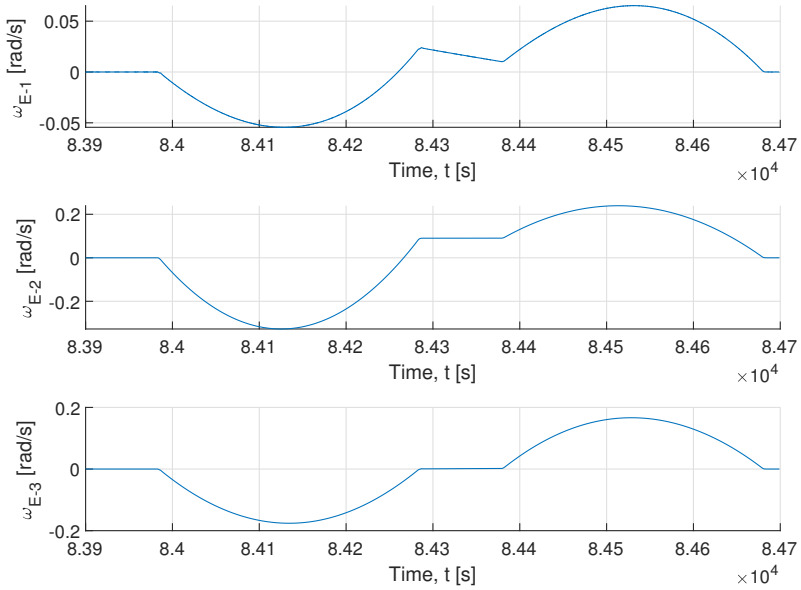

Figure 6.10: Angular rate error, 1^{st} reaction wheel failed

The behavior is almost the same compared the nominal case, showing that the controller does not suffer the effect of actuators failure during the mission. However, the simulation shows the same problematic of the nominal case.

The second case is shown in the following figures:

Everything told for the first case applies for case concerning the second reaction wheel failed. The behavior is like the nominal case, even for what concern the errors.

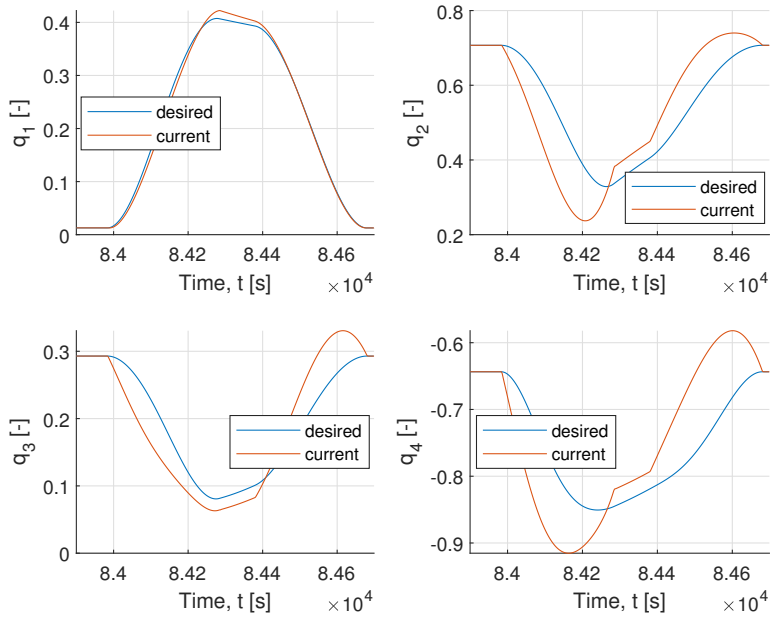

Figure 6.11: Quaternions, 2^{nd} reaction wheel failed

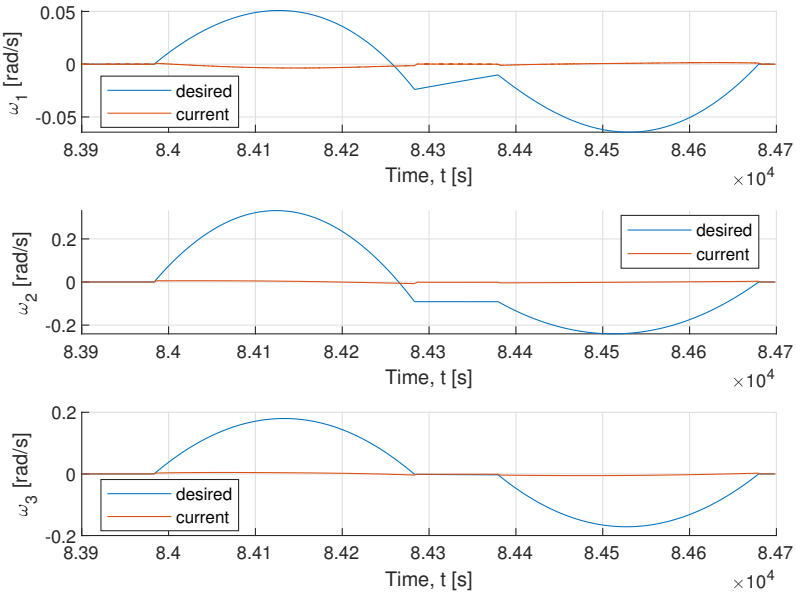

Figure 6.12: Angular rate, 2^{nd} reaction wheel failed

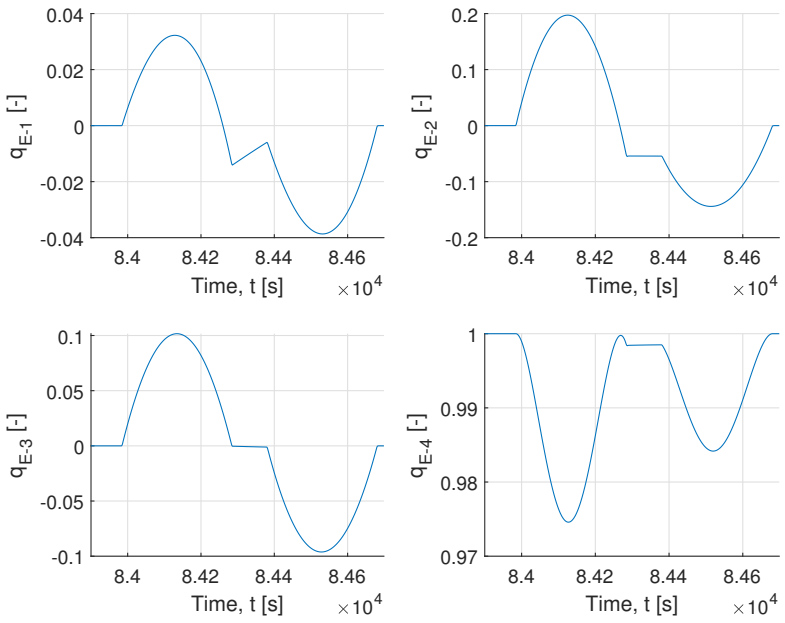

Figure 6.13: Quaternion error, 2^{nd} reaction wheel failed

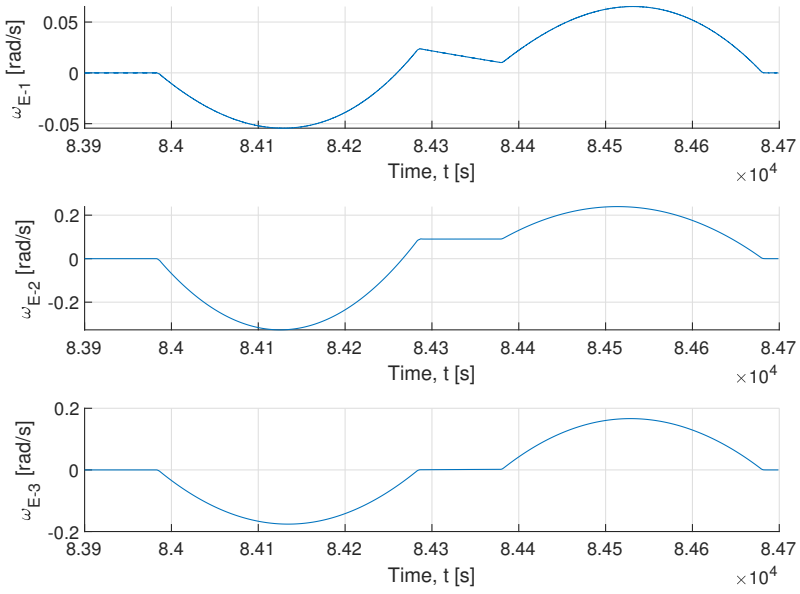

Figure 6.14: Angular rate error, 2^{nd} reaction wheel failed

The case considering the third reaction wheel failed is presented and analyzed as it follows in figure 6.15.

The third case is almost the same of the previous case, no differences can be seen. The errors are still important in the transitional phases, while slower in the scientific phase. This proves the capability of the controller to work even in case of failures.

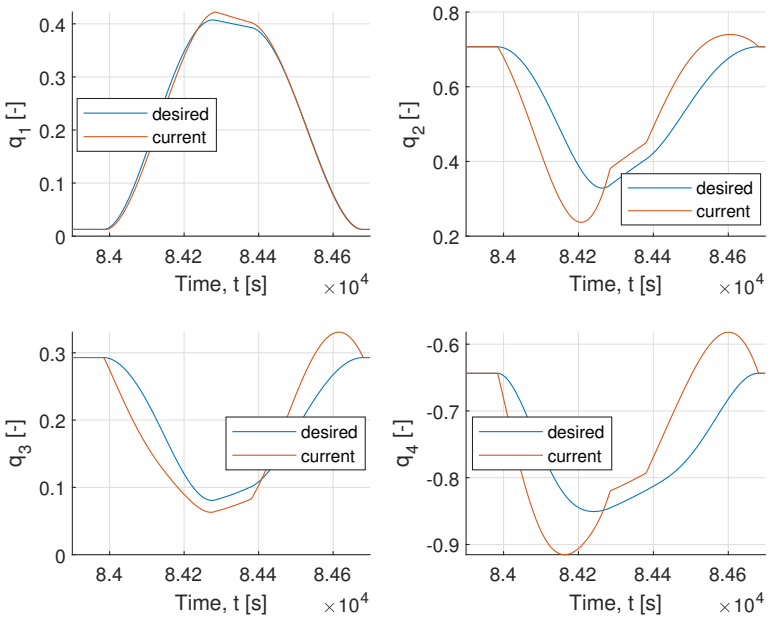

Figure 6.15: Quaternions, 3^{rd} reaction wheel failed

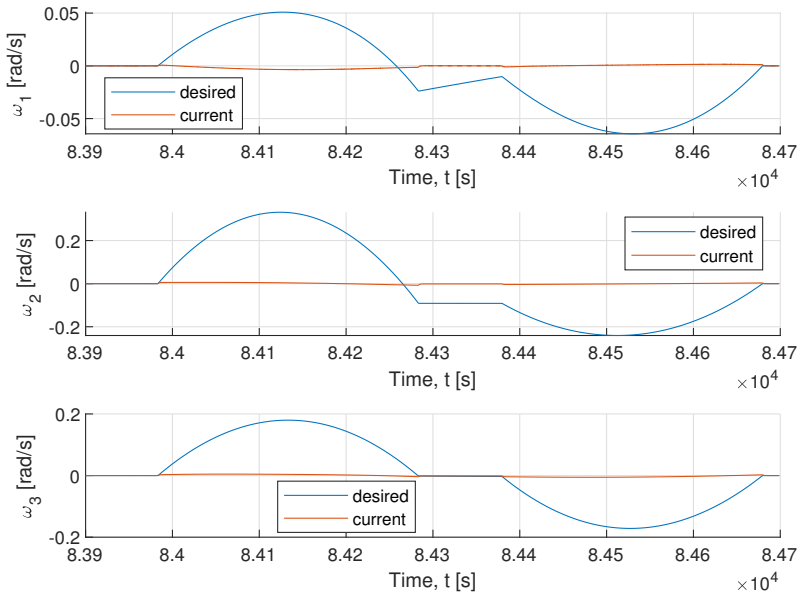

Figure 6.16: Angular rate, 3^{rd} reaction wheel failed

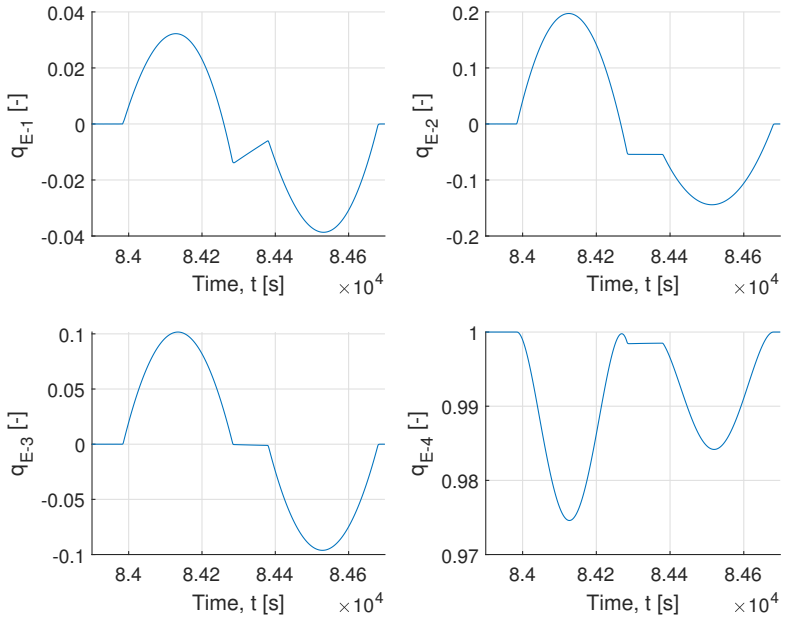

Figure 6.17: Quaternion error, 3^{rd} reaction wheel failed

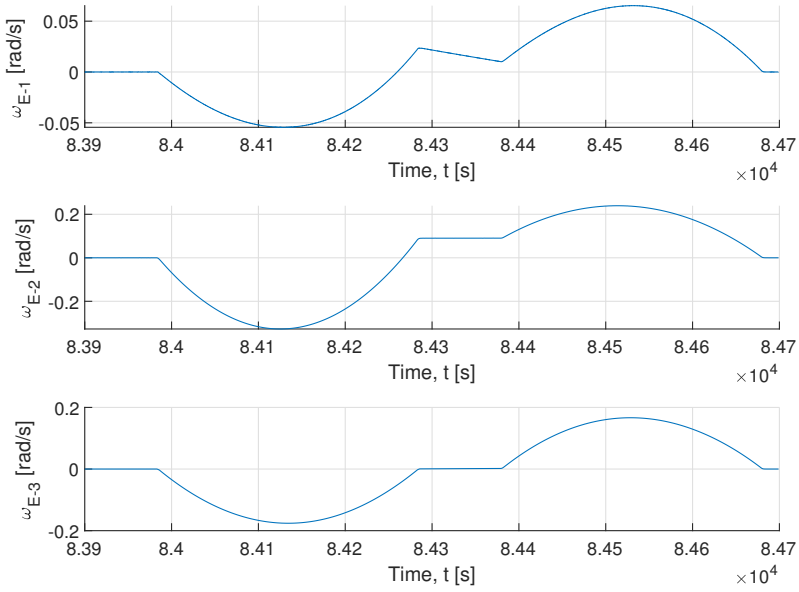

Figure 6.18: Angular rate error, 3^{rd} reaction wheel failed

The last case, the one with the fourth reaction wheel failed is shown in figure6.19.

This simulation shows almost the same behavior seen in the previous cases. The variations of quaternions and angular rates are quite the same, as the errors as well.

To sum up, it is possible to notice that the behavior of these cases is similar, showing that the controller is not affected by the failure. However, the existing quaternion and angular rate errors, almost the same for each case, can be important and unneglectable. Every case shows a well behaviour for the quaternion q_1, while for the other quaternions q_2, q_3 and q_4 show an overshooting problem.
More specifically, the nature of the resultant error can be interpreted as the controller inability to follow exactly the desired configuration during the transitional phase of the mission, i.e. where the satellite changes its configuration from the starting one to the desired one. In fact, when the satellite should be operating the error is acceptable, less than 7 degree for the worst-case scenario.

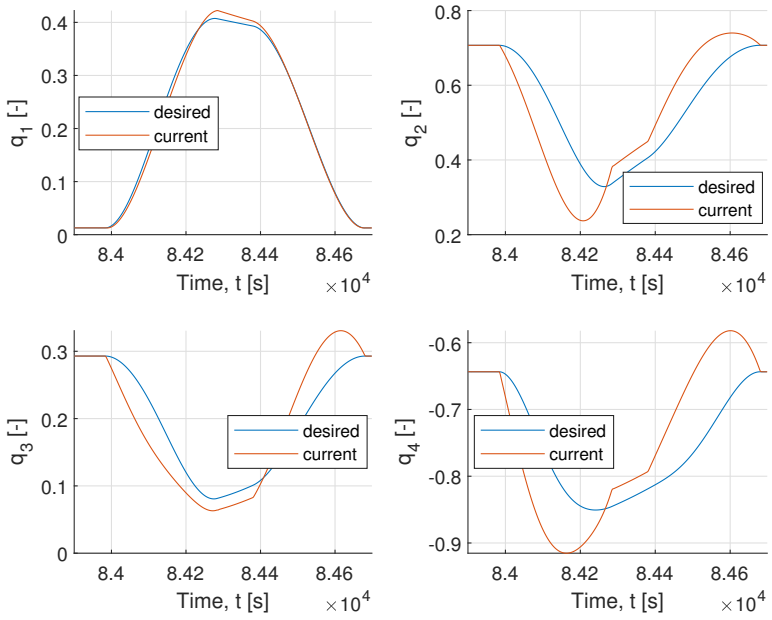

Figure 6.19: Quaternions, 4^{th} reaction wheel failed

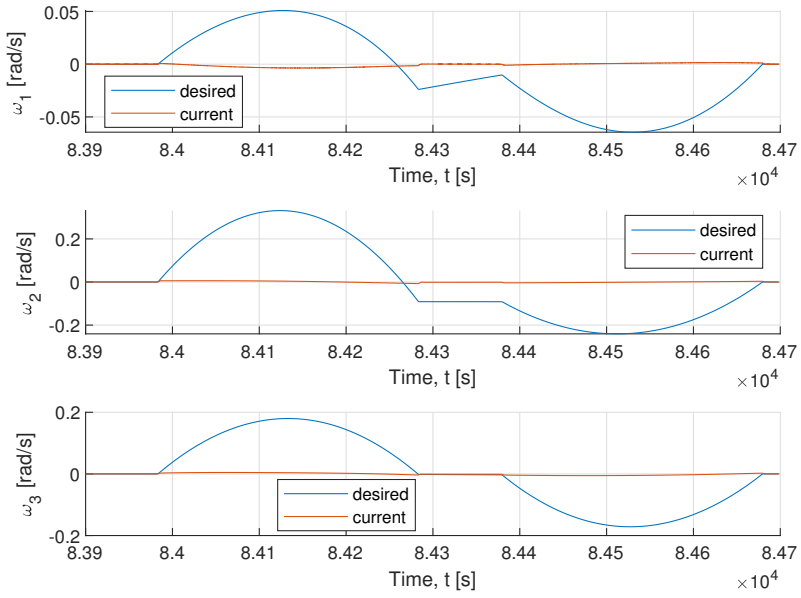

Figure 6.20: Angular rate, 4^{th} reaction wheel failed

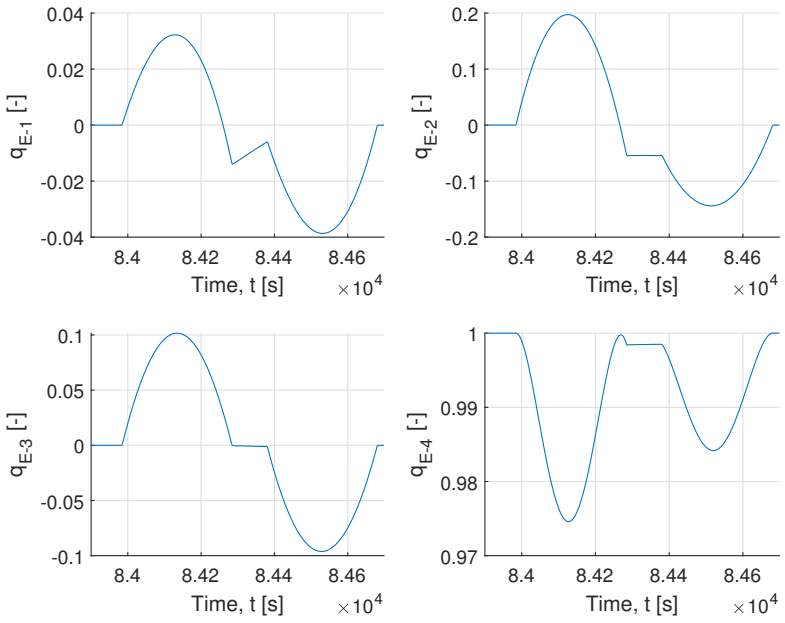

Figure 6.21: Quaternion error, 4^{th} reaction wheel failed

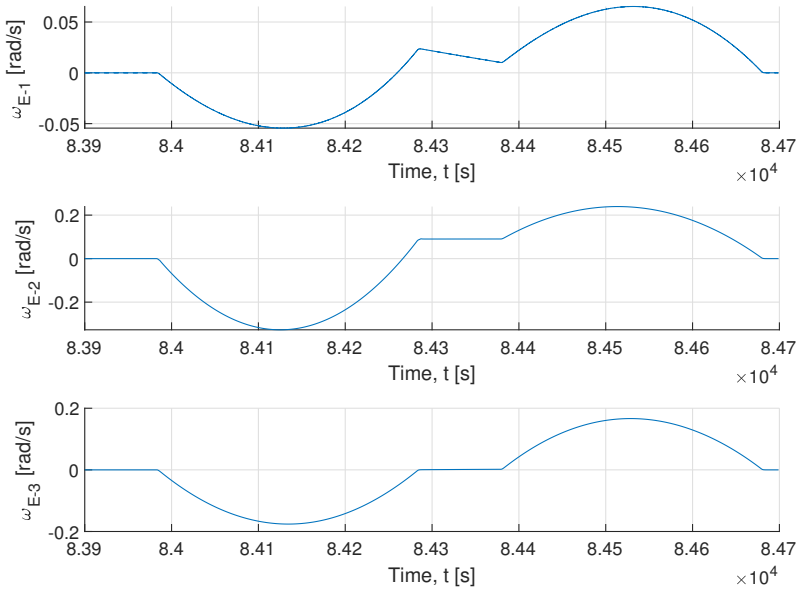

Figure 6.22: Angular rate error, 4^{th} reaction wheel failed

Chapter 7

Conclusion & Future works

In conclusion, this work of thesis can be summed up in three main topics: H_∞ controller, Fault Detection method and the mission scenario.
In the first part of the thesis, the attitude control system is presented. An H_∞ controller is designed through a mathematical optimization of the LMIs problem. Through the robustness that characterizes this kind of controllers, it has been possible to work with uncertainties within the plant and with a reaction wheel failure. In fact, with an assumption about the weights of each reaction wheel, the failure was considered as an uncertainty. The final design shows a *unique* state-feedback K controller for both uncertainties.
Then, a fault detection method based on parity equations is designed. Two MED systems are considered, where the only difference between them is the allocation matrix: one is varying according the failure and the other is always equal to the nominal case. If the two systems show some discrepancy, it means the system is affected by a failure. This method, eventually, shows the health of each reaction wheel.
Finally, a mission scenario is tested with the previously designed H_∞ controller implemented with the fault detection system. The controller shows a good behavior against the failures, as their presence do not produce any significant difference. However, during the transition part of the mission, the error can be important, but during the scientific part is lower within acceptable margin of operation.
In the future, several improvements can be done to achieve a greater level of exhaustiveness of this project.
Firstly, a fault detection method more advanced than the one used in this thesis can be achieved. For example, it could be a good idea to implement some methods based on machine learning or artificial intelligence, that nowadays are gaining more attention by researchers.
Secondly, as the last chapter emphasises, the current controller can achieve the desired configuration but the behavior cannot be handled as detailed as a PID controller, showing thus some difficulties to tune the controller. Therefore, it may be necessary to re-design an H_∞ controller that can be tuned more easily.
Eventually, Monte Carlo simulations, based on the Chernoff bound, may be done to verify the designed approach.

Bibliography

[1] V.D. Kuznetsov, V.M. Sinelnikov, S.N. Alpert b, *Yakov Alpert: Sputnik-1 and the first satellite ionospheric experiment*, Advances in Space Research, Volume 55, Issue 12, Pages 2833-2839, 15 June 2015.

[2] NASA, *Voyager 1 Reaches Interstellar Space*, URL: `https://science.nasa.gov/science-news/science-at-nasa/2013/12sep_voyager1`, accessed in March 2019.

[3] NASA, Solar system exploration, *NASA's Voyager 2 Probe Enters Interstellar Space*,URL: `https://solarsystem.nasa.gov/news/784/nasas-voyager-2-probe-enters-interstellar-space/`, accessed in March 2019.

[4] G. Facchinetti, *SMALL SATELLITES, Economic Trends*, Master dissertation, Universita' Commerciale Luigi Bocconi, Milano, Italy, December 2016.

[5] M. Wall, *SpaceX Rocket Makes Historic 3rd Launch Into Space with 64 Satellites On Board*, URL `https://www.space.com/42599-spacex-falcon-9-rocket-3rd-launch-success-sso-a.html`, December 3 2018. Accessed in March 2019.

[6] ISRO, *PSLV-C37 Successfully Launches 104 Satellites in a Single Flight* `https://www.isro.gov.in/update/15-feb-2017/pslv-c37-successfully-launches-104-satellites-single-flight`, February 15 2017. Accessed in March 2019.

[7] G. Zames, *Feedback and optimal sensitivity: Model reference transformations, multiplicative seminorms, and approximate inverses*. IEEE Transactions on Automatic Control. 26 (2): 301–320.(1981)

[8] J. W. Helton, *Orbit structure of the Mobius transformation semigroup action on H-infinity (broadband matching)*. Adv. Math. Suppl. Stud. 3: 129–197. (1978)

[9] A. Tannenbaum, *Feedback stabilization of linear dynamical plants with uncertainty in the gain factor*. International Journal of Control. 32 (1): 1–16. (1980).

[10] K. Zhou, J. C. Doyle, *Essentials of Robust Control*, Prentice hall, 1998.

[11] D.Arzelier, (2008), *LMIs in systems control state-space methods performance analysis and synthesis.Course on LMI optimization with application in control. Part II.2*[pdf]. URL: `https://homepages.laas.fr/arzelier/polycop/dea/commande_etat2.pdf`

[12] D. Overbye, *Breakdown Imperils NASA's Hunt for Other Earths*, New York Times, URL: https://www.nytimes.com/2013/05/16/science/space/equipment-failure-may-cut-kepler-mission-short.html

[13] Y. M. Zhang and J. Jiang, *Bibliographical review on reconfigurable fault-tolerant control systems*, Annual Reviews in Control, vol. 32, no. 2, pp. 229–252, 2008.

[14] A. Zhang, Y. Wang, Z. Zhang, and H. R. Karimi, *Robust Control Allocation for Spacecraft Attitude Stabilization under Actuator Faults and Uncertainty*,Hindawi Publishing Corporation, Mathematical,Problems in Engineering, Volume 2014, Article ID 789327, 12 pages. 13 February 2014.

[15] Y. Bai, J. D. Biggs, X. Wang, N. Cui, *Attitude tracking with an adaptive sliding mode response to reaction wheel failure*, European Journal of Control 42 (2018) 67–76.

[16] Sir W. R. Hamilton, *On Quaternions; or on a new System of Imaginaries in Algebra*, The London, Edinburgh and Dublin Philosophical Magazine and Journal of Science, 1844–1850.

[17] S. R. Crews II, *Increasing slew performance of reaction wheel attitude control systems*, Master of Science dissertation, September 2013. pp. 165(187)-166(188).

[18] O. Sename, *Robust and LPV control of MIMO systems. Part 2: H_∞ control*[pdf]. Gipsa-lab, Tecnologico de Monterrey, June 2016.

[19] MOSEK ApS, *The MOSEK optimization toolbox for MATLAB manual. Version 8.1.*, URL:http://docs.mosek.com/8.1/toolbox/index.html,2017.

[20] J. Löfberg, *YALMIP : A Toolbox for Modeling and Optimization in MATLAB*,In Proceedings of the CACSD Conference, Taipei, Taiwan,2004.

[21] D. Miljković, *Fault Detection Methods: A Literature Survey*, MIPRO 2011, May 23-27, 2011, Opatija, Croatia.